REPORT DOCUMENTATION PAGE

Form Approved
OMB No. 0704-0188

1. REPORT DATE *(DD-MM-YYYY)*	2. REPORT TYPE	3. DATES COVERED *(From - To)*
02-01-2013	FINAL	01-09-2009 TO 30-09-2012

4. TITLE AND SUBTITLE

Oxidation Resistance of Alloys from Nb-Si-Cr System for High Temperature Applications

5a. CONTRACT NUMBER

5b. GRANT NUMBER
N00014-09-1-1070

5c. PROGRAM ELEMENT NUMBER

6. AUTHOR(S)

5d. PROJECT NUMBER
10PR04001-00

5e. TASK NUMBER

5f. WORK UNIT NUMBER

7. PERFORMING ORGANIZATION NAME(S) AND ADDRESS(ES)

The University of Texas at El Paso
Admin Bldg, room 209
El Paso, TX 79968

8. PERFORMING ORGANIZATION REPORT NUMBER

9. SPONSORING / MONITORING AGENCY NAME(S) AND ADDRESS(ES)

Office of Naval Research
875 North Randolph Street
Arlington, VA 22203-1995

10. SPONSOR/MONITOR'S ACRONYM(S)
ONR 332

11. SPONSOR/MONITOR'S REPORT NUMBER(S)

12. DISTRIBUTION / AVAILABILITY STATEMENT

David A. Shifler

20130109225

13. SUPPLEMENTARY NOTES

14. ABSTRACT

This project was a research and education grant from ONR. The total period for the grant was 5 years. The purpose is to explore alloys from Nb based alloys for high temperature applications and involves undergraduate and graduate students in this educational component. The main aim for students education was to generate interest in students to pursue higher education for undergraduate students while prepare the graduate students for professional careers in research (at one of the ONR facilities). Outcomes: 8 undergraduate and 8 graduate students completed the program. All the undergraduate students are enrolled in institutions to continue their graduate studies (either M.S. or Ph.D.). One of them is in France to work on his Ph.D. degree. All the graduate students are currently professional individuals at places such as Halliburton, Alcoa Gas Company in Oklahoma etc. One of them owns a silver mine in Mexico and is conducting the extraction of silver from the ores. The results of this research have been published in refereed journals throughout the tenure of this grant. It is the policy of this research that graduate students must have a peer reviewed publication before they can defend their M.S. theses or Ph.D. dissertations which indicate the authored names. Journal of Materials Science, Metallurgical and Materials Transactions A, Corrosion Science and Journal Alloys and compounds are a few examples where results have been published. Students were also asked to make

15. SUBJECT TERMS

16. SECURITY CLASSIFICATION OF:			17. LIMITATION OF ABSTRACT	18. NUMBER OF PAGES	19a. NAME OF RESPONSIBLE PERSON
a. REPORT	b. ABSTRACT	c. THIS PAGE		47	Dr. Shailendra Varma
					19b. TELEPHONE NUMBER *(include area code)* (915) 747-6937

SUMMARY

This project was a research and education grant from ONR. The total period for the grant was 5 years. The purpose is to explore alloys from Nb based alloys for high temperature applications. The education component deals with the undergraduate and graduate students. The main aim for students education was to generate interest in students to pursue higher education for undergraduate students while prepare the graduate students for professional careers in research (at one of the ONR facilities). It was possible for 8 undergraduate and 8 graduate students to complete the program. The attempt to achieve the objective was largely achieved. All the undergraduate students are enrolled in institutions to continue their graduate studies (either M.S. or Ph.D.). One of them is in France to work on his Ph.D. degree. All the graduate students are currently professional individuals at places such as Halliburton, Alcoa Gas Company in Oklahoma etc. One of them owns a silver mine in Mexico and is conducting the extraction of silver from the ores.

The research component was the exploration of Nb-Cr-Si-Mo-B system and understanding the role of Cr and Si (ternary system) on the oxidation resistance in air from 700 to 1500°C. Nb-Cr-Si-Mo-B system was developed to the stage where a claim can be made that it is possible to come up with a composition which can last for 2 weeks of continuous heating in air up to a temperature of 1300°C. Thus far the Nb-25Cr-20Mo-15Si-15B alloy exhibits outstanding oxidation resistance in air in this temperature range. Nb-rich solid solution was has been found to deteriorate the oxidation resistance but is needed for toughness in this system. It has been observed that B addition can reduce the amount of this phase and is still a topic of continuing research at this institution. Kathryn Thomas is a Ph.D. student who is conducting this study.

Nb-Cr-Si was studied by holding the Cr concentration to 25 atomic percent and varying the Si from 10 to 42 atomic percents. The CR concentration was held to 25 atomic percent because this study in the initial phase concluded that exceeding Cr from beyond this results in detrimental effects on oxidation resistance. The Si was varied based on the ternary isothermal sections computed from a Pandat™ computer program. A 42 percent Si has demonstrated exception oxidation resistance up to 1400°C due to the presence of two uncommon silicides whose presence has been rather ignored in the literature. However, the excellent oxidation resistance is confined to only 24 hour heating period in air. It is proposed that a study be

conducted to determine the resistance up to 2 weeks like the other system studied in this program. There was not enough time to perform such experiments.

The results of this research have been published in refereed journals throughout the tenure of this grant. All publications have the names of students as primary or coauthor. It is the policy of this research that graduate students must have a peer reviewed publication before they can defend their M.S. theses or Ph.D. dissertations. Journal of Materials Science, Metallurgical and Materials Transactions A, Corrosion Science and Journal Alloys and compounds are a few examples where results have been published. Students were also asked to make technical presentations in national and international conferences at a professional level. This was considered as part of the education component of this grant.

It must be pointed out that equipments like high temperature furnaces, ion mills, electro polishing units, DTA, microbalance and dimpler have been acquired by the compliments of this ONR grant. These equipments are being used by the students of this department for further research in this or other research topics.

Nb-25Cr-20Mo-15Si-xB System

The effect of adding B to Nb-25Cr-20Mo-15Si alloys has been determined. The purpose of this study was to explore the possibility of forming a borosilicate scale which has been shown to very successful in alloys from Mo-Si-B system. Monolithic form of this alloy was alloyed with 5, 10, and 15 atomic percent boron for this study.

Figure 1 shows the isothermal sections of the Nb-Cr-Mo-Si phase diagram at 700 and 1300°C as calculated by the PANDAT^{TM} software program. It clearly indicates the chosen composition of this study is expected to have a microstructure consisting of $NbCr_2$ Laves phase, Nb_5Si_3, and α Nb solid solution. It also indicates that no phase transformation is to be expected from 700 to 1300°C indicative of the microstructural stability.

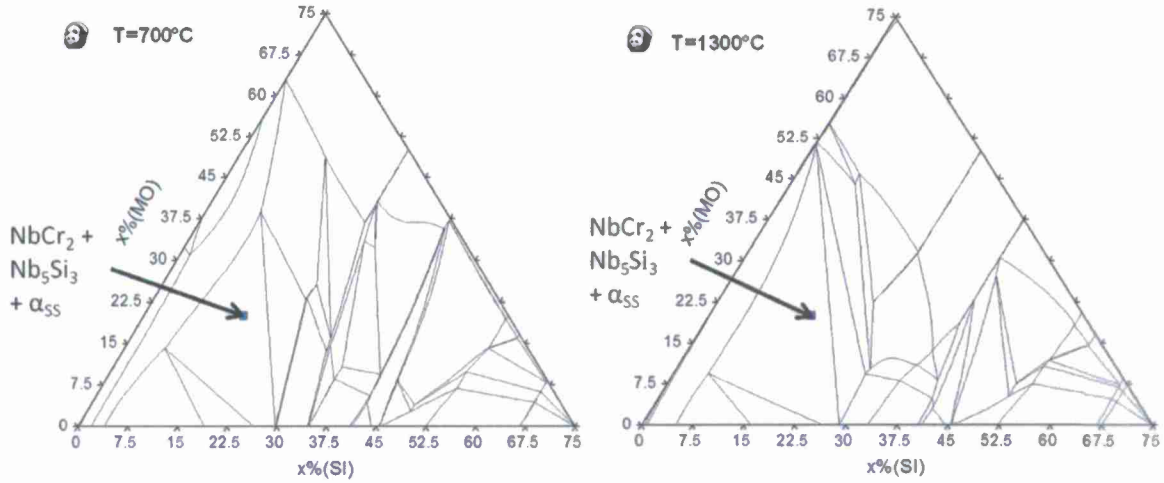

Figure 1 Isothermal sections at 700 and 1300°C for Nb-Cr-Mo-Si phase diagram. Sections were made at temperatures intervals of 100°C from 700 to 1300°C (not shown here). They indicate that no isothermal section is to be expected in this temperature range. B effect is not shown due to database limitations.

Figure 2 shows the actual microstructures for all the 4 alloys. 25Cr alloy shows the primary α solid solution islands in a matrix of eutectic like microconstituent consisting of eutectic α, $NbCr_2$ and Nb_5Si_3 (5-3 silicide). $NbCr_2$ is present as both in primary and eutectic forms. The eutectic like structure is quite fine in the as cast condition. An addition of 5B to 25Cr alloy reduces the amount of primary α significantly but still contains a rather coarser eutectic like microconstituent. A Nb_3Si (3-1 silicide) silicide phase is also seen in 5B alloy. It must be

noted that this phase was not predicted by the calculated isothermal sections and it did not appear anywhere else in this any of the 4 alloys studied in this research. A sharp interface between this and eutectic like microconstituent may be an indication of a coherent boundary. Another important feature for 5B alloy includes the appearance of primary form of 5-3 silicide.

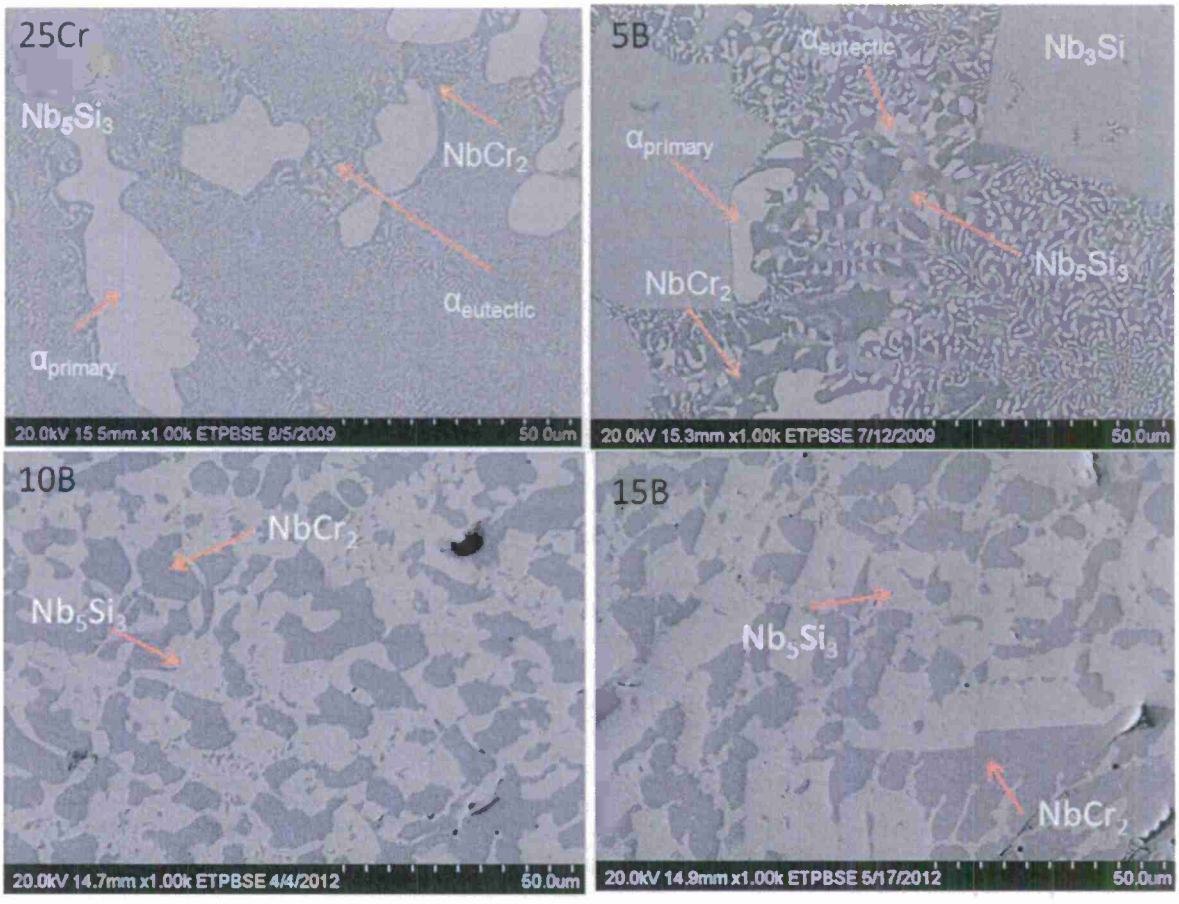

Figure 2 As-cast microstructures of the Nb-25Cr-20Mo-15Si (25Cr alloy), Nb-25Cr-20Mo-15Si-5B (5B alloy), Nb-25Cr-20Mo-15Si-10B (10B alloy), and Nb-25Cr-20Mo-15Si-15B (15B alloy) alloys.

The 10B alloy begins to show a very distinct and different microstructure in the sense that the primary α and eutectic like phases have almost completely disappeared while primary 5-3 silicide and $NbCr_2$ phases dominate the microstructure along with some eutectic like phases. However, the 15B alloy shows no evidence of either primary α or eutectic like structures. Thus

the only difference between 10 and 15B alloy is the minute amount of eutectic like microconstituent in 10B alloy.

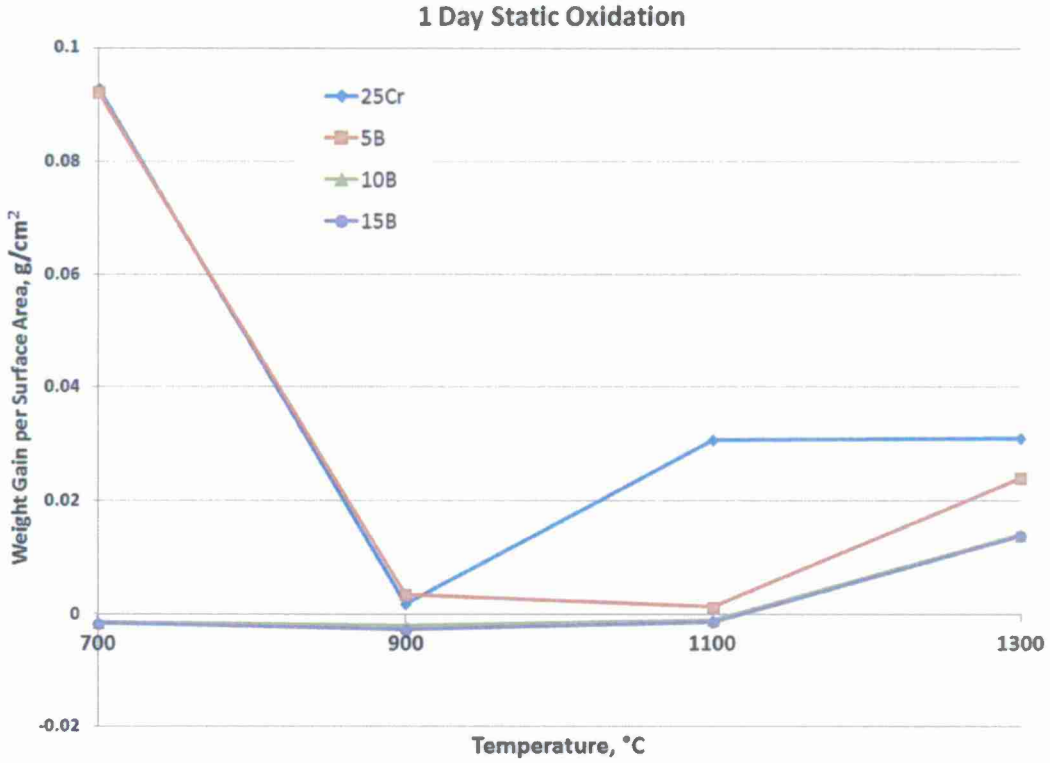

Figure 3 Oxidation curves for 25Cr, 5B, 10B, and 15B alloys from 700 to 1300°C.

B alloys were then exposed to laboratory air for 24 hours in a range of temperatures from 700 to 1300°C followed by furnace cooling to room temperature. The weight before and after heating provides weight gain per unit area which is then plotted as a function of oxidation temperature to yield oxidation curve. Figure 1 shows the oxidation curves for 25Cr, 5B, 10B and 15 B alloys. Both 25Cr and 5B alloys suffer from extensive low temperature pesting at 700°C as seen by a rather large value of weight gain in Figure 3. However, the beneficial effect B addition is clearly seen at 1100 and 1300°C. This study indicates that the curves for 10B and 15B alloys appear to be almost overlapping at these four temperatures.

More importantly, Figure 4 shows that the amount of metal left in the crucible is almost 100% meaning that barely any oxidation occurred even at high temperatures of 1100 and 1300°C. This shows a very significant improvement in oxidation resistance by the B addition to 25Cr alloy. Figure 4 is a cyclic oxidation curve which is a graph between weight gain per unit

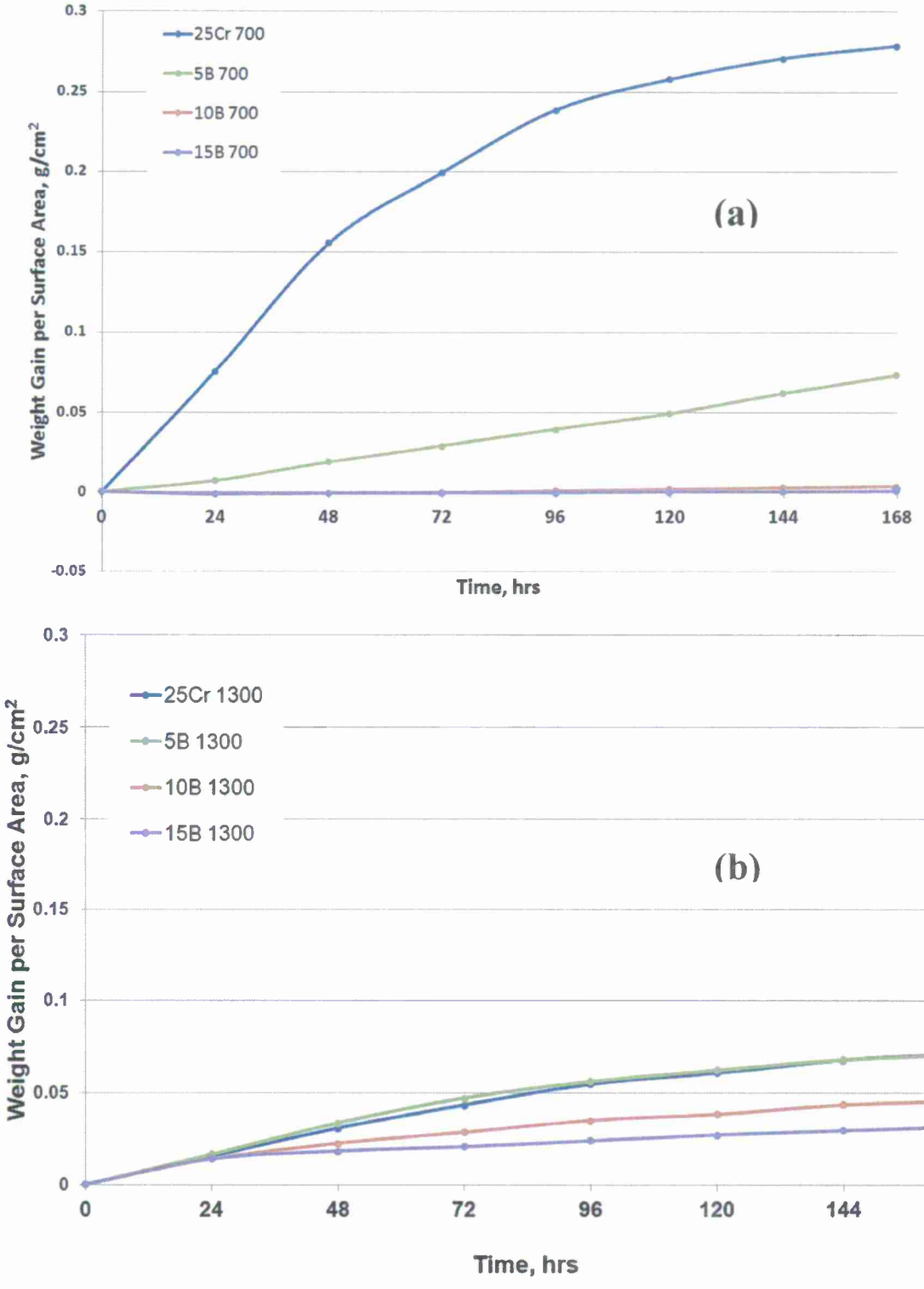

Figure 4 (a) Cyclic oxidation curves for 25Cr, 5B, 10B, and 15B alloys at 700°C for a period of one week or 168 hours. (b) Below is the cyclic curve at 1300°C.

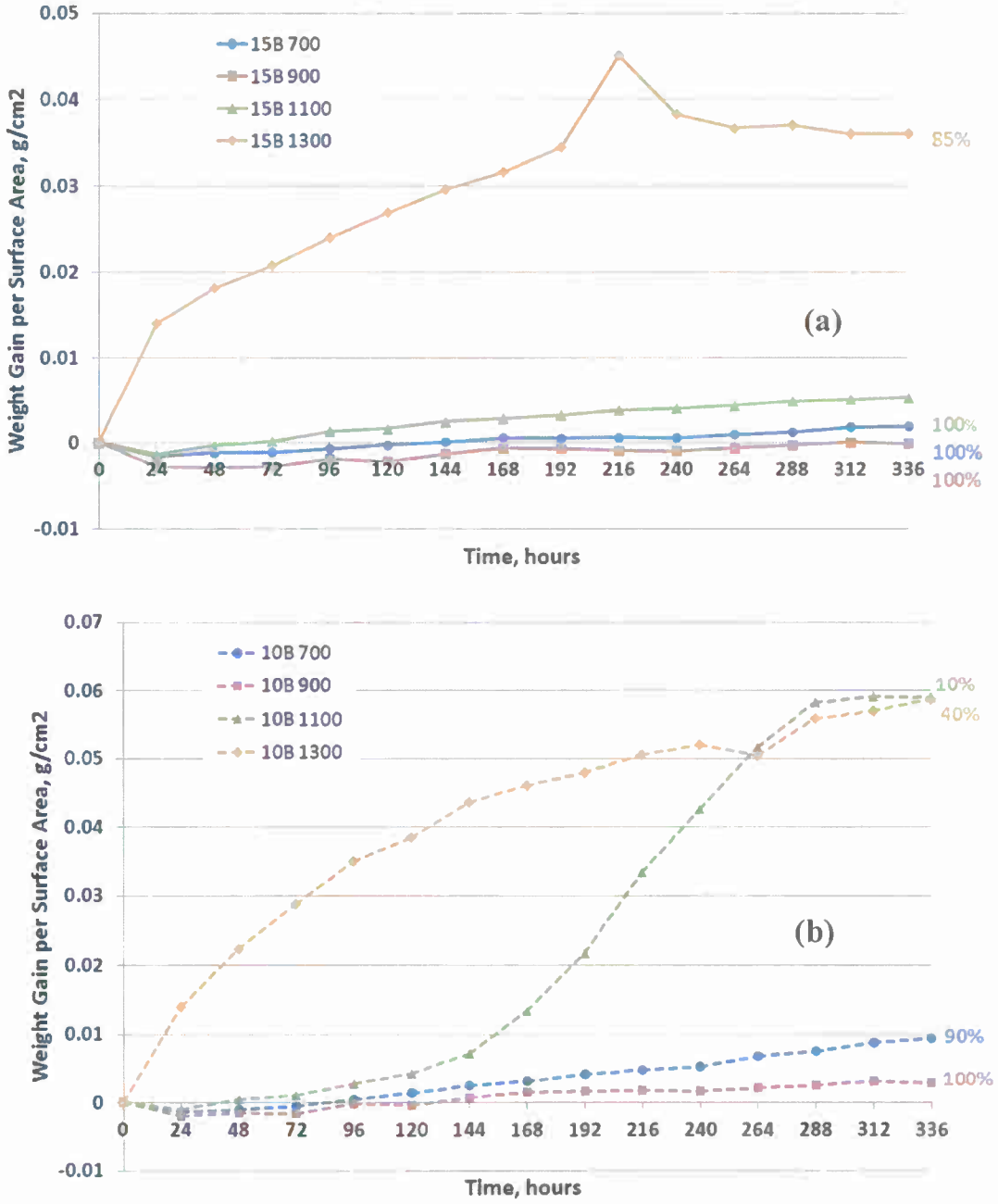

Figure 5 (a) Cyclic oxidation curves for 25Cr, 5B, 10B, and 15B alloys at 700°C for a period of two weeks or 336 hours. (b) Below is the cyclic curve at 1300°C.

area as a function of oxidation time at a given temperature. Both 25Cr and 5B alloys clearly point to a weight loss of measurable extent. Figure 4(b) shows the cyclic curves at 1300°C for all the alloys. The presence of 70 and 90% of the metal left for 10 and 15B alloys is considered

as remarkable. It points to the fact that 15B alloy is capable of retaining 90% of the metal even after oxidizing it for one week or 168 hours at 1300°C.

Thus it can be summarized that main advantage of adding B to 25Cr alloy may consist of (a) reduced porosity, (b) significant reduction of pesting, (c) elimination of a phase and even eutectic like phases with 15B addition, and (d) elimination of bulky oxide formation typical of 25Cr alloy especially in the range from 900 to 1100°C.

Two weeks cyclic oxidation curves are shown in Figure 5. The graph, Figure 5(a), showing curves at 700°C shows that 10B alloy although has 100 and 90% retained metal at 900 and 700°C, respectively, still contains 40% metal left at 1300°C. The shape of the curve for 1100°C is questionable. Figure 5(b), on the other hand, shows very promising results for 15B alloy. The 15B alloy can sustain 336 hours of oxidation in air at 1300°C. This is considered as outstanding oxidation resistance for Nb based alloys. Lower temperature oxidations have almost no loss of metal for 15B alloy.

XRD patterns of the oxidized products for 10 and 15B alloys after oxidation at 700, 900, 1100, and 1300°C are shown in Figure 6. Both alloys oxidize to produce similar oxides: $CrNbO_4$ and Monoclinic form of Nb_2O_5. However, trace amounts of SiO_2 can also be detected in the patterns especially for 15B alloy at higher temperatures. There two important aspects which must be noted. First, these alloys only show monoclinic form of Nb_2O_5 only which is a high temperature form above 1100°C. The form of Nb_2O_5 which is harmful for Nb alloys is the intermediate temperature form and it has a crystal structure of base centered monoclinic. This is the form which produces a bulky oxide in the range of temperature from 900 to 1100°C and has been observed to oxidize very quickly which results in catastrophic oxidation in Nb alloys in the intermediate temperature range. The low temperature form has orthorhombic crystal structure. It is possible to conclude that B addition to the alloy suppresses the formation of base centered monoclinic form of Nb_2O_5. Second, the presence of Si first as SiO_2 and free or combined Si which may be present as amorphous or crystalline form. It will be shown later that both SiO_2 and amorphous Si may be present. Amorphous form provides low viscosity so it makes the scale more dense and difficult for oxygen to penetrate through it to reach the base metal for oxidation. $CrNbO_4$ is considered as a very beneficial oxide which can act as a protective layer if formed in sufficient quantity. The observation in this study does not point to the formation of a continuous film of this oxide.

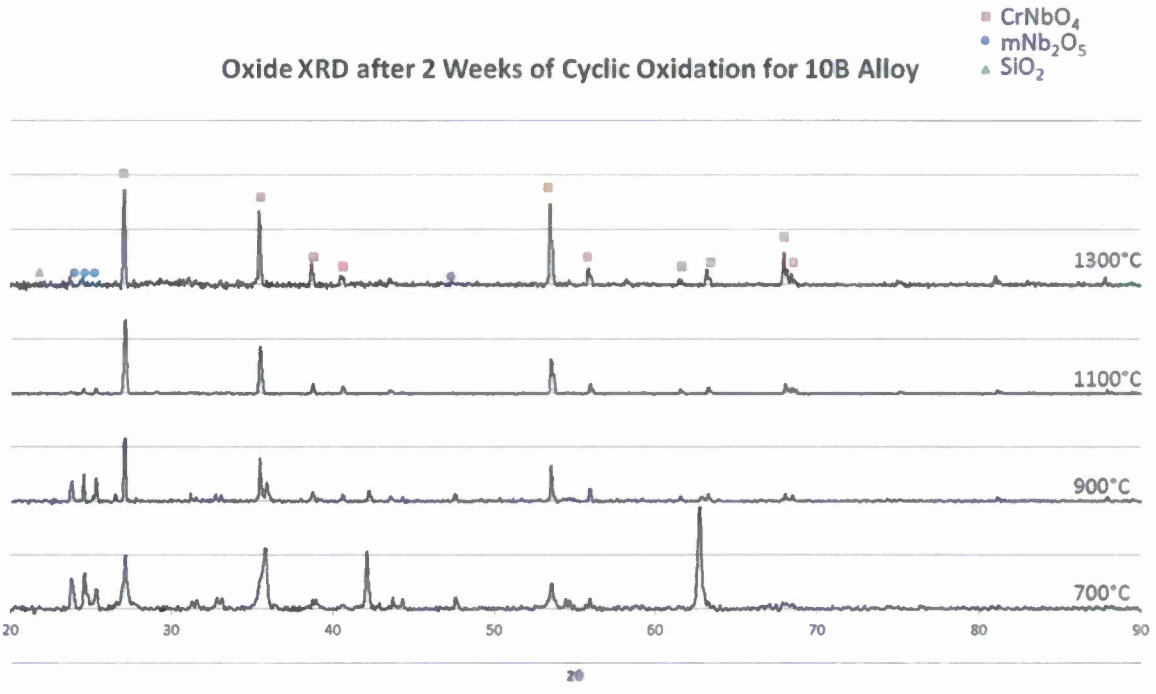

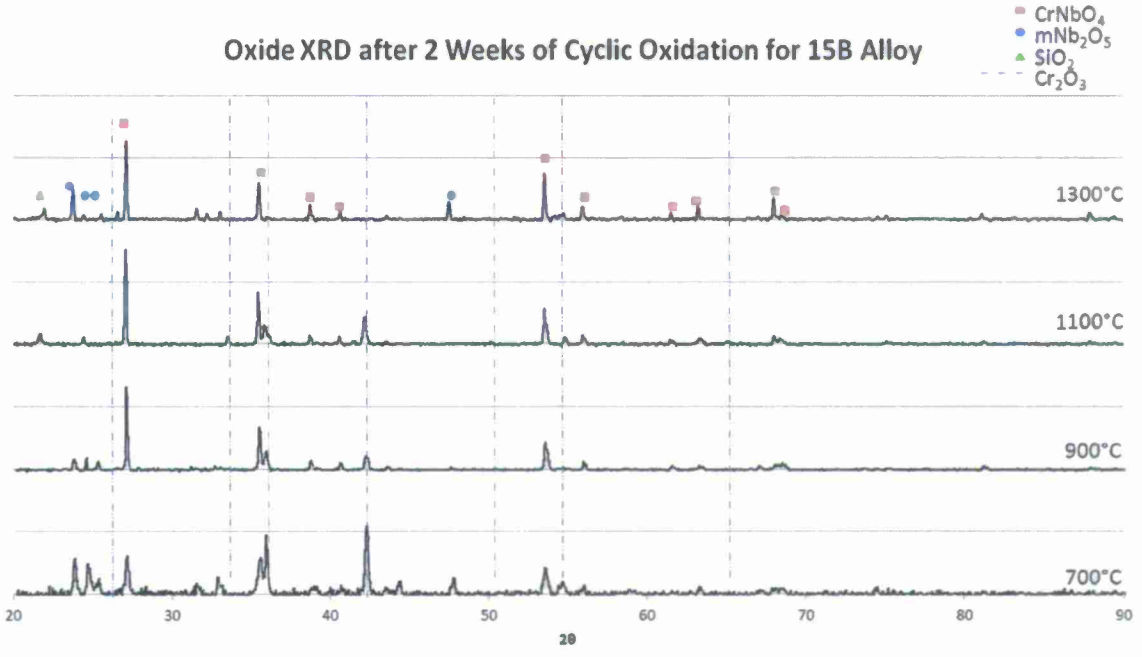

Figure 6. XRD patterns of the oxidized products for 10B and 15B alloys at 700, 900, 1100, 1300°C are shown here after 2 weeks.

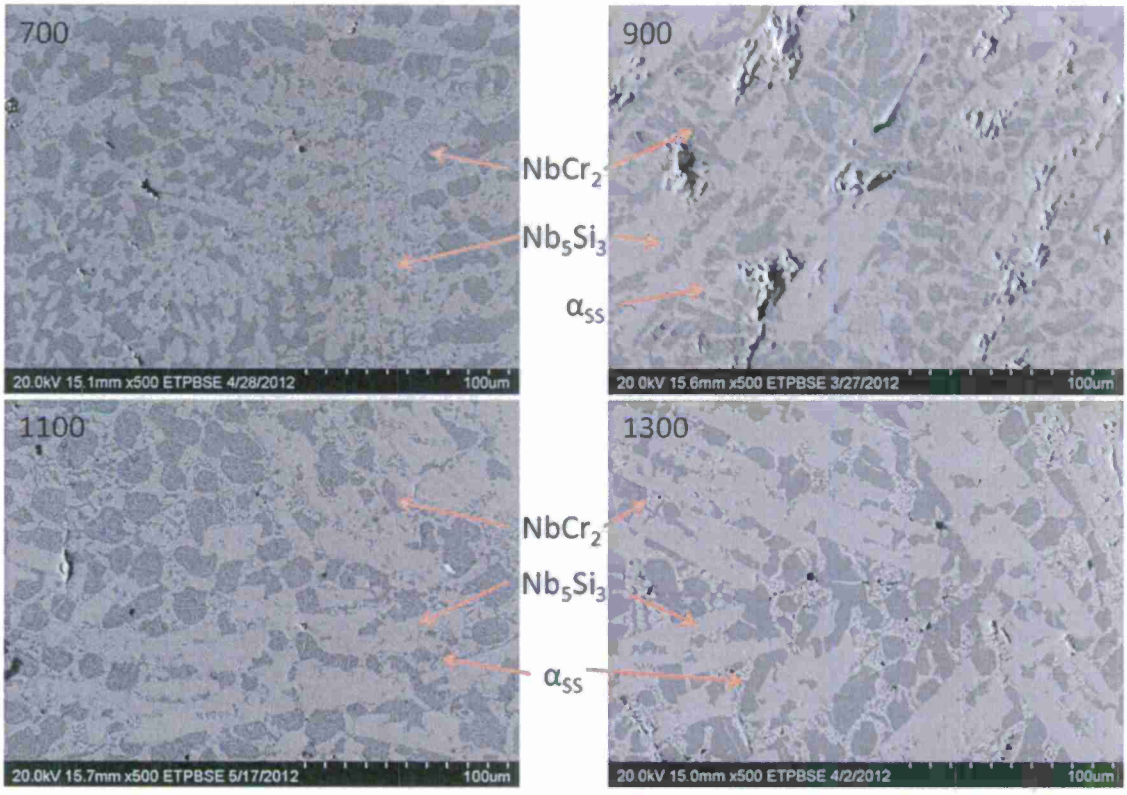

Figure 7 Microstructures for the 10B alloy after 2 weeks of oxidation at the indicated temperatures.

Microstructural stability of the alloys has been tested by examining the base metal after oxidation at different temperatures. Figure 7 shows it for 10B alloy at 700, 900, 1100, and 1300°C. These microstructure must be compared to the as cast structure shown in Figure 2. Significant changes can be noticed only at 1100 and 1300°C. A higher amount of eutectic like structure is present at 1100°C and only isolated example of the presence of primary α can be seen. Besides this there is not other change that can be observed from Figure 7. Rather noticeable amount of primary α can be seen at 1300°C.

Figure 8 shows the microstructural stability for 15B alloy. It can be seen that this alloy exhibits excellent microstructure stability since there is no change from what was observed in the as-cast condition as was shown in Figure 2(d). The only change observed is the coarsening of the structure which is to be expected. Obviously it must be concluded that 15B alloy not only shows the best oxidation resistance of the 4 alloys studied in this research but it can also withstand the

microstructures without degradation which can be extremely useful for the high temperature mechanical properties.

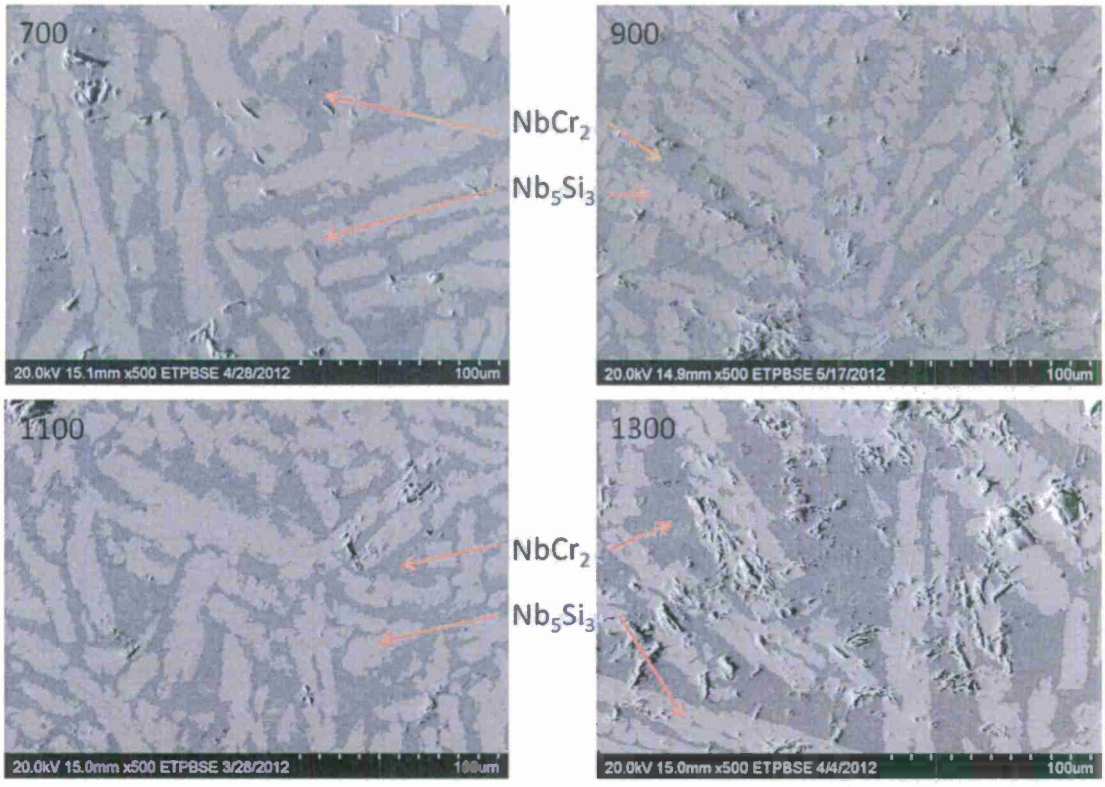

Figure 8 Microstructures for the 15B alloy after 2 weeks of oxidation at the indicated temperatures.

The oxide-metal (OM) microstructure after oxidation at 700, 900, 1100 and 1300°C for 10 B alloys is shown in Figure 9. Large amount porosity in the scale has been observed at 700°C resulting in appreciable amount of pesting. The scale adhesion to the alloy surface is also not very good at this temperature. A thin layer developed at 900°C which lies between the alloys surface and the oxide scale and is being referred to intermediate oxidation layer (IOL). It comprises of $CrNbO_4$, Nb_2O_5, and SiO_2. IOL begins developed progressively with an increasing oxidation temperature as shown in the OM microstructures at 1100 and 1300°C in Figure 8. Porosity seems to be decreasing at higher oxidation temperatures and x-ray mapping indicates that the IOL is depleted in Cr while it is enriched with Mo. The presence of Mo is then assumed to be in the form of its oxides or in solid solution form. There is evidence to indicate certain amount of spalling taking place particularly noticeable at 1300°C.

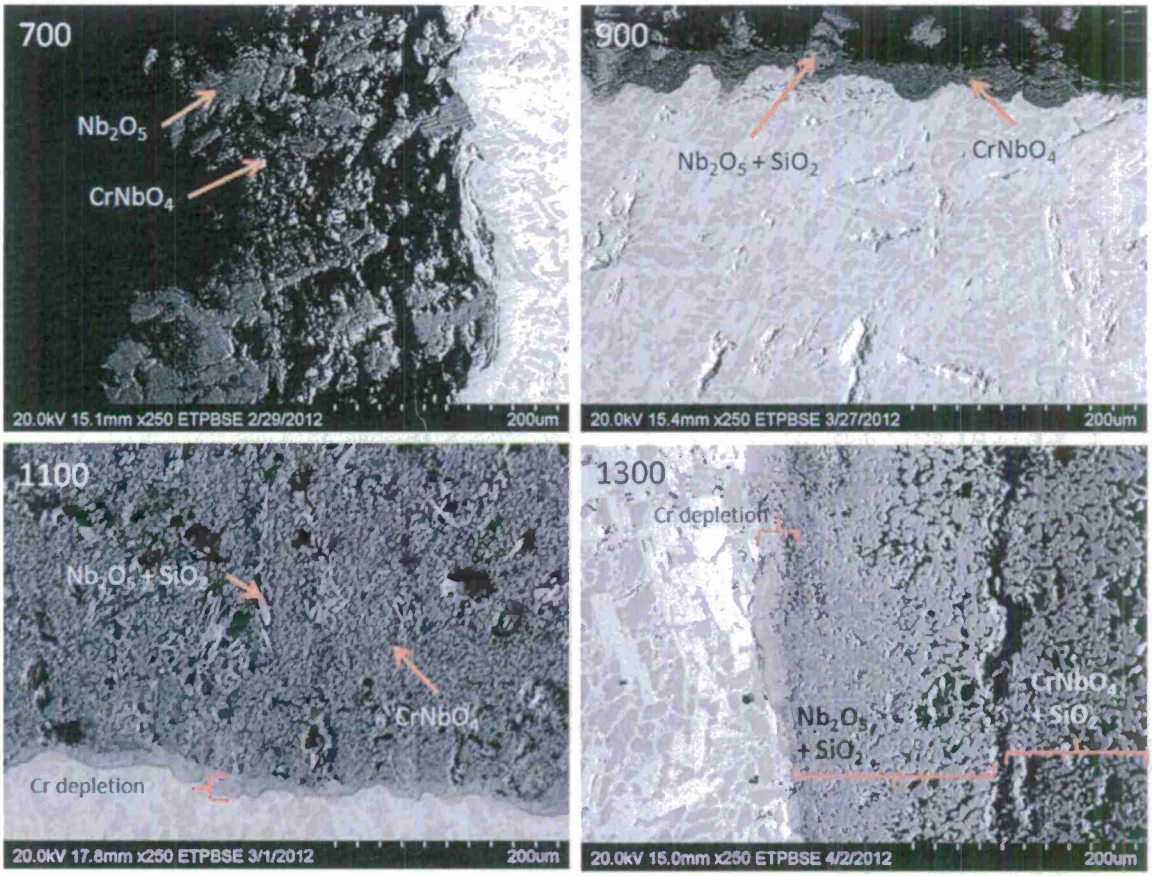

Figure 9. Oxide-metal interface structure for 10B alloy after oxidation at 700, 900, 110, and 1300°C for 2 weeks in air.

The OM microstructure for 15B alloy is shown in Figure 10. Even though the porosity continues to develop at 700 and 900oC the IOL development is very pronounced for this alloy. $CrNbO_4$ and SiO_2 mixture dominates the scale structure but the IOL not only sharpens but also becomes thicker. Large voids in the scale can be seen at 1300oC in Figure 10. Cr depleted and Mo enriched IOL is clearly marked for identification purposes. Another striking feature of IOL is the retention of morphology of the microconstituents from the matrix after oxidation. The reason for this IOL feature is not well understood at this time. However, it must be repeated that the IOL offers extremely good oxidation resistance to the alloy. In a way it appears that it acts like a protective layer which prevents the easy flow of oxygen from air to the alloy for oxidation to continue. It believed that B may be responsible for this beneficial feature shown by B alloys in general. Nevertheless, its formation is very desirable.

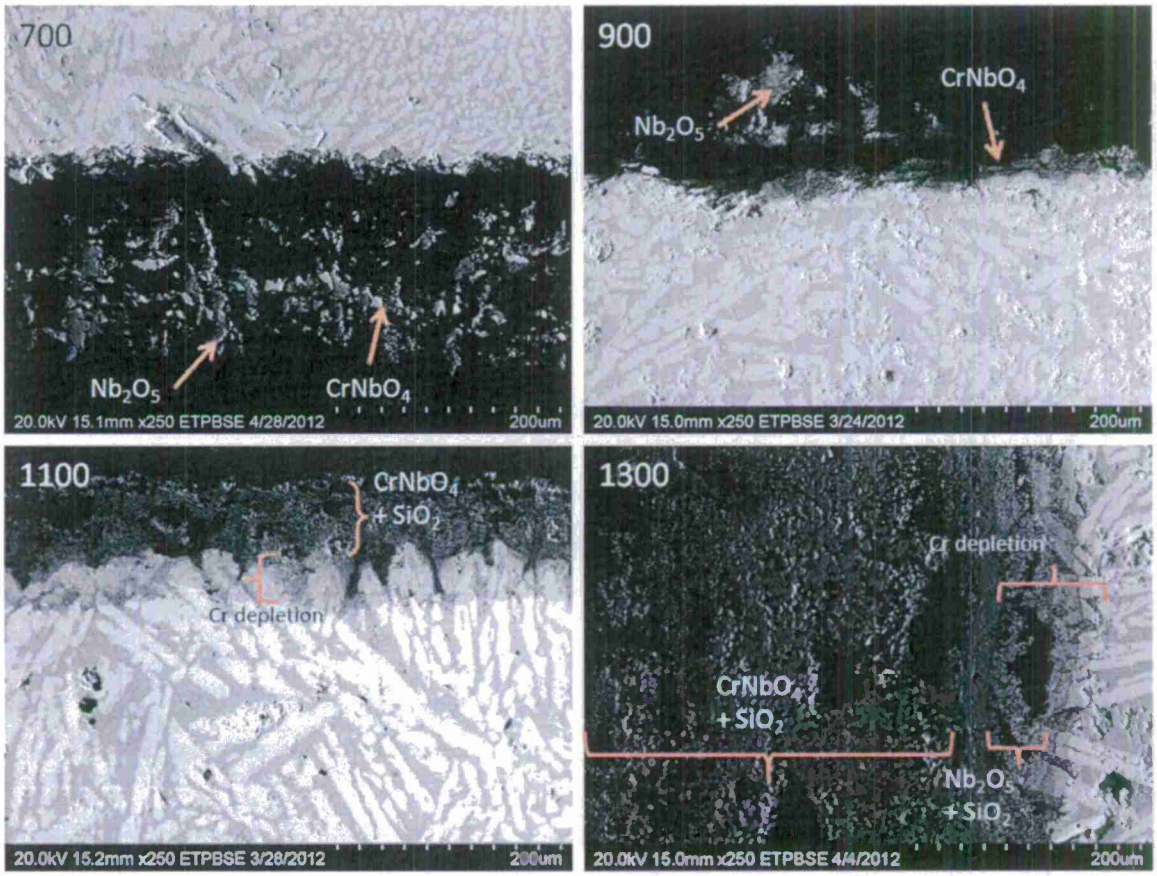

Figure 10. Oxide-metal interface structure for 15B alloy after oxidation at 700, 900, 110, and 1300°C for 2 weeks in air.

A comparison for the 2 week oxidation in air between the 10 and 15B alloys may be seen in the following table:

Nb25Cr-20Mo-15Si-10B Alloy	Nb25Cr-20Mo-15Si-15B Alloy
Less porous	Porosity is visible but could be inhibited by HIP processing.
Microstructure shows some instability with some Nb_{ss} forming at 900°C.	Stable microstructure at all temperatures
Pest oxidation still occurs at low oxidation temperatures.	Only minute amount of pesting was observed at 1300°C.
Thin IOL at 1100 and 1300°C.	Well developed IOL by 1100°C.
This oxide scale at 1100 and 1300°C.	Thick scale only at 1300°C.
Greater weight gain at high temperatures.	Large weight gain only at 1300°C.

A comparison between static and cyclic oxidation has been made in this study. A 2 week cyclic heating will involve the heating for a period of 2 weeks but in 24 heating cycles. It means that the sample is heated at a given temperature for 24 hours cooled down to room temperature and heated again after recording the weight gain. However, static heating, on the other hand, would involve the heating continuously for 2 weeks without any interruptions.

Figure 11 shows static oxidation curves for 10 and 15B alloys for 3 days (72 hours) of heating at 700, 900, 1100, and 1300°C. The curves show excellent oxidation resistance at these temperatures. Even with a severe static heating at these temperatures, the amount of metal left in the crucible is especially noticeable. It ranges from 90 to almost 100% across this entire temperature range which is outstanding behavior for a Nb alloy. In fact, the amount of metal left is 98 or 100% at 700, 900, and 1100°C. It is only at 1300oC that it shows 90 and 95% for 15 and 10B alloy respectively. The advantage of adding 15B versus 10B to the alloy is vividly shown in Figure 11. Weight gain per unit area is also well within the limits of acceptable range in comparison to nickel base superalloys.

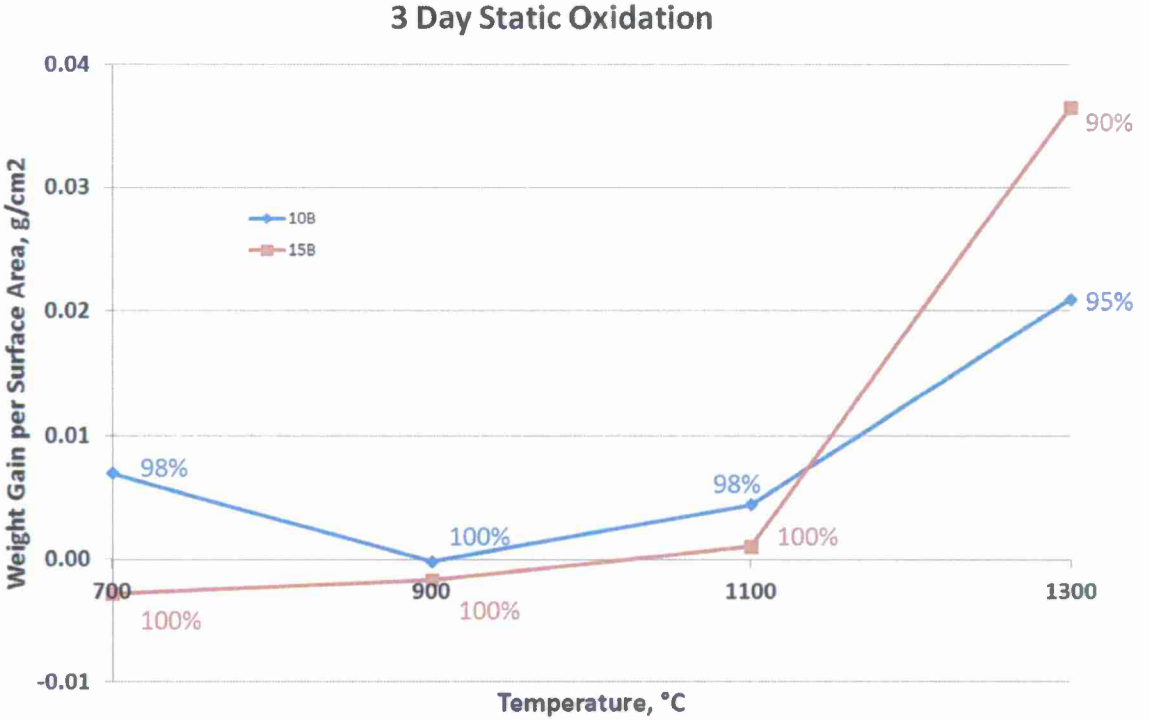

Figure 11. Isothermal oxidation curves for 10 and 15B alloys at 700,900, 1100, and 1300°C after heating (static) the alloy continuously for 3 days or 72 hours.

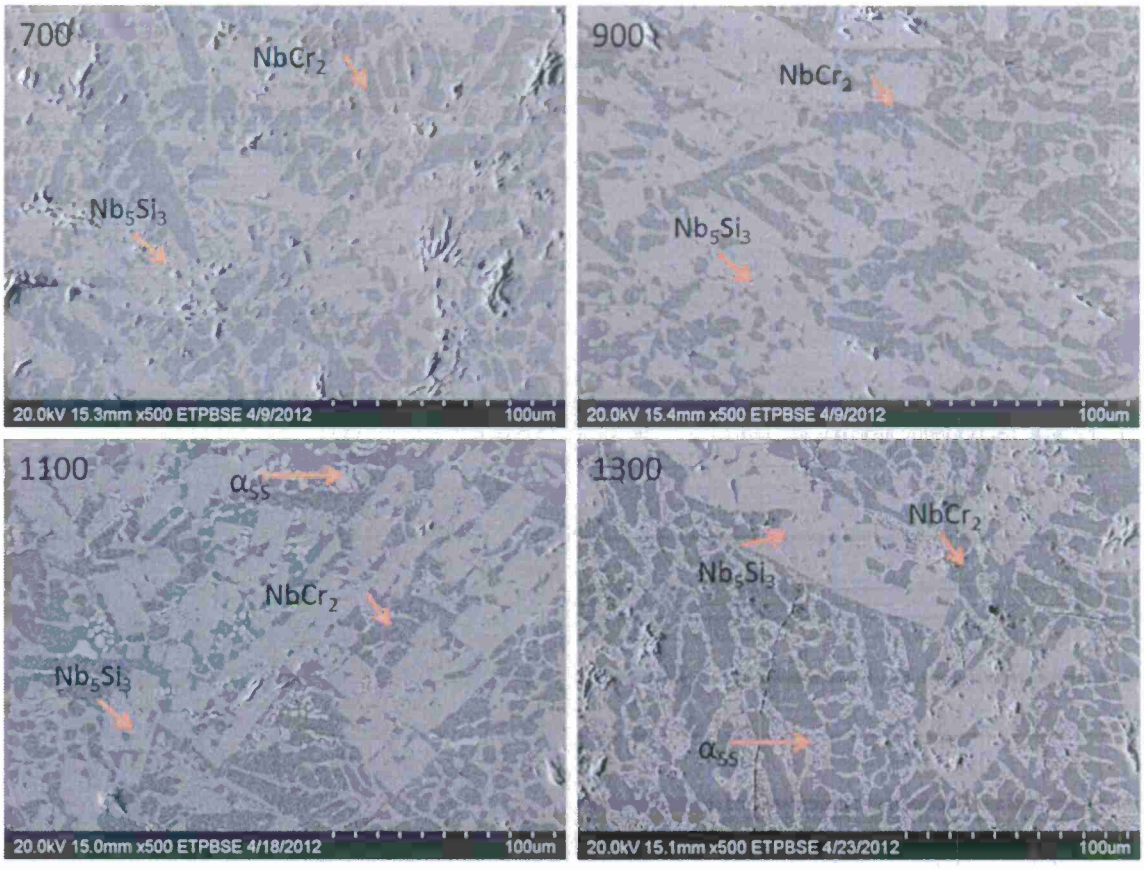

Figure 12. Microstructural Thermal stability observation for 10B alloys after 3 days of static oxidation in air at 700, 900, 1100, and 1300°C.

The stability for microstructures after 3 days static oxidation in air at 700, 900, 1100 and 1300oC is shown in Figure 12. This microstructure is to be compared with the microstructure shown in the as cast condition for 10B alloy as shown in Figure 2. It can be seen that α_{ss} phase begins to appear at 900°C in the microstructures while a distinct eutectic like microconstituent develops at 1100°C. Of course, the α_{ss} phase is also present in the eutectic like microconstituent. It clearly points to the fact that the microstructure is fairly stable in this temperature. Even better microstructural thermal stability is exhibited by the 15B alloy as show in Figure 13. This alloy shows no break-up of the microstructural features at all. The two phases remaining up to 1300oC are simply 5-3 silicides and Laves phases. As before the only effect of heating that can be seen is the coarsening which is to be expected. Laves phase distribution remains unaffected by the

oxidation process and the 5-3 silicide almost appear to form a basis for matrix for the alloy although it has not been verified quantitatively.

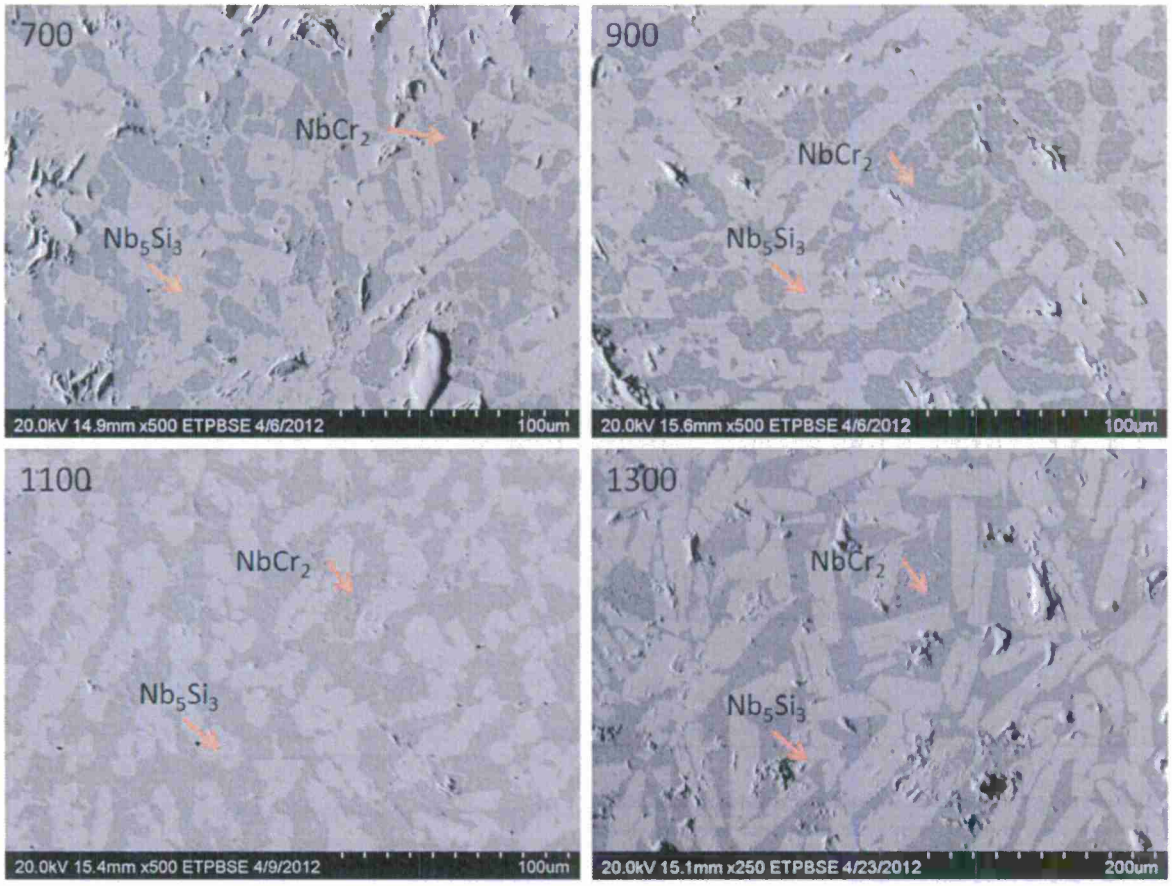

Figure 13. Microstructural Thermal stability observation for 15B alloys after 3 days of static oxidation in air at 700, 900, 1100, and 1300°C.

It is very surprising to see the results of XRD patterns for the oxidation products shown in Figure 14. A comparison with the XRD patterns after 2 weeks of cyclic oxidation with Figure 6 shows identical patterns. There are no signs of Nb_2O_5 transformation to its other allotropic forms which an indication that undesirable base centered monoclinic form is certainly not formed in the system. Only the high temperature monoclinic form was detected along with $CrNbO_4$. Only a trace amount of SiO_2 was seen. But the presence Si by x-ray mapping again points to the fact the Si may actually be present in amorphous form. The reader is referred to the discussion on this topic in the earlier part of this report. Cr_2O_3 has been observed only low temperatures at 700 and 900°C. It must be noted that oxide of Cr is nto unstable at very high

temperatures used in this study. It is safe to assume that Cr is involved in the oxidation process by the formation of $CrNbO_4$.

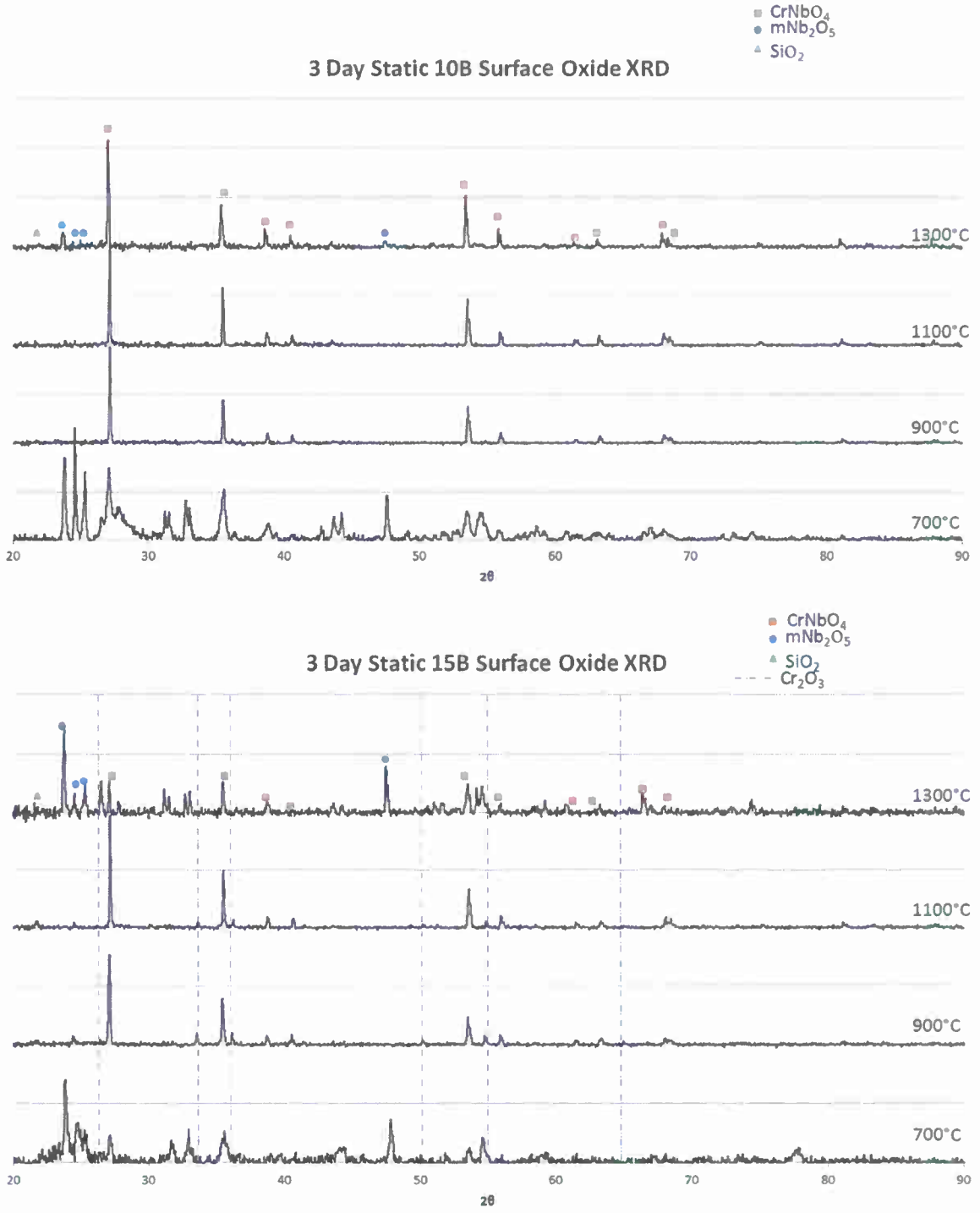

Figure 14. XRD for the oxidation products developed at 700, 900, 1100, and 1300°C oxidation after 3 days static heating in air for 10B (top figure) and 15B (bottom figure).

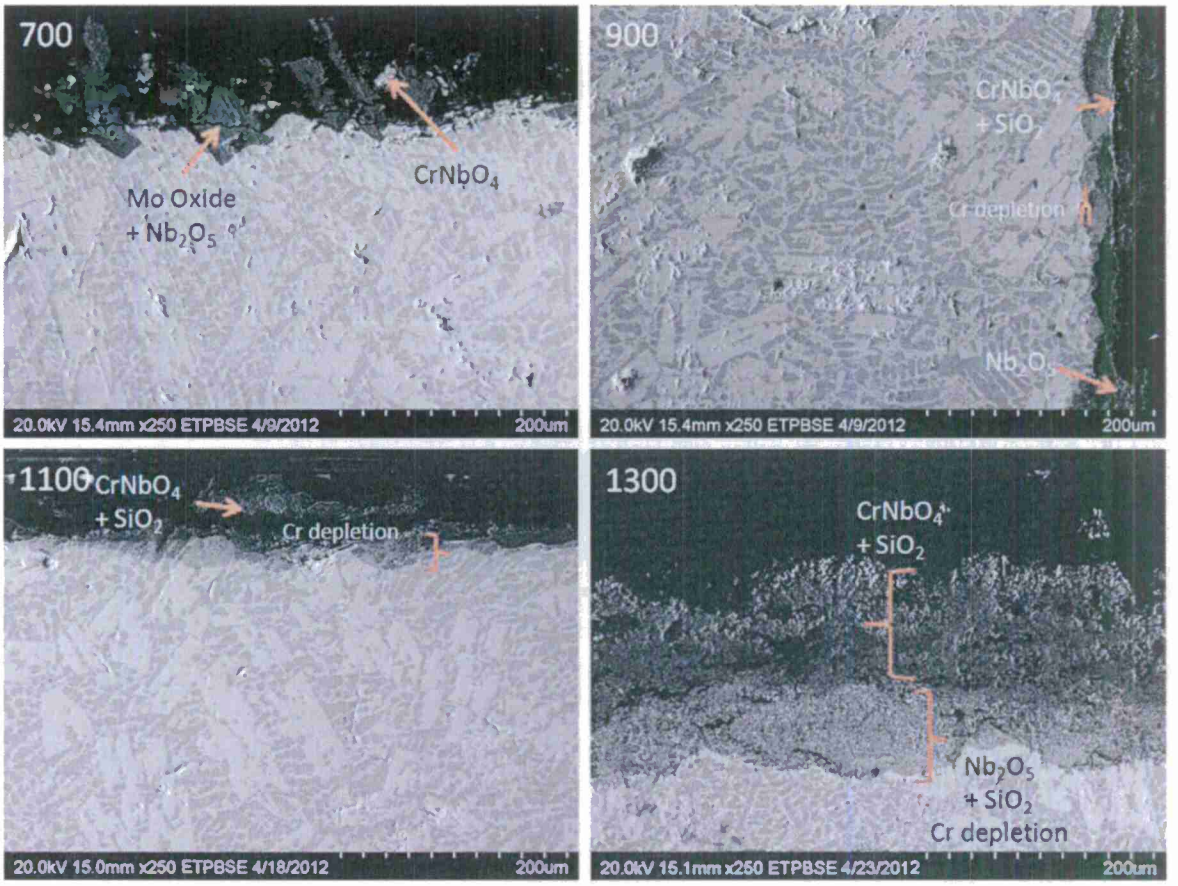

Figure 15. The Oxide-Metal structure of 10B alloy after oxidation at 700, 900, 110, and 1300°C for 3 day static oxidation.

The structure oxide-metal interface for 10B alloy is shown in figure 15 after the alloy has been subjected to 3 day static oxidation in air at 700, 900, 1100, and 1300°C. It can be seen that almost patchy like oxidation takes place at 700°C while a continuous layer of oxide has been observed at 900°C. In fact, the IOL formation is quite identifiable at 900°C. A white layer on top of the IOL layer consists of $CrNbO_4$ and SiO_2 along with patches of Nb_2O_5. However, the IOL identification is clearly seen at 1100°C. The x-ray maps helps to identify the locations of the oxides and Figure 16 shows for the 3 day static oxidation of 10B alloy at 1300°C. One of the striking characteristic of the layer is the depletion of Cr and enrichment of Mo in it. However,

immediately above the IOL the scale is outlined with $CrNbO_4$ with a SiO_2 matrix. Mo also appears to be more or less uniformly distributed in the oxide scale just as Nb.

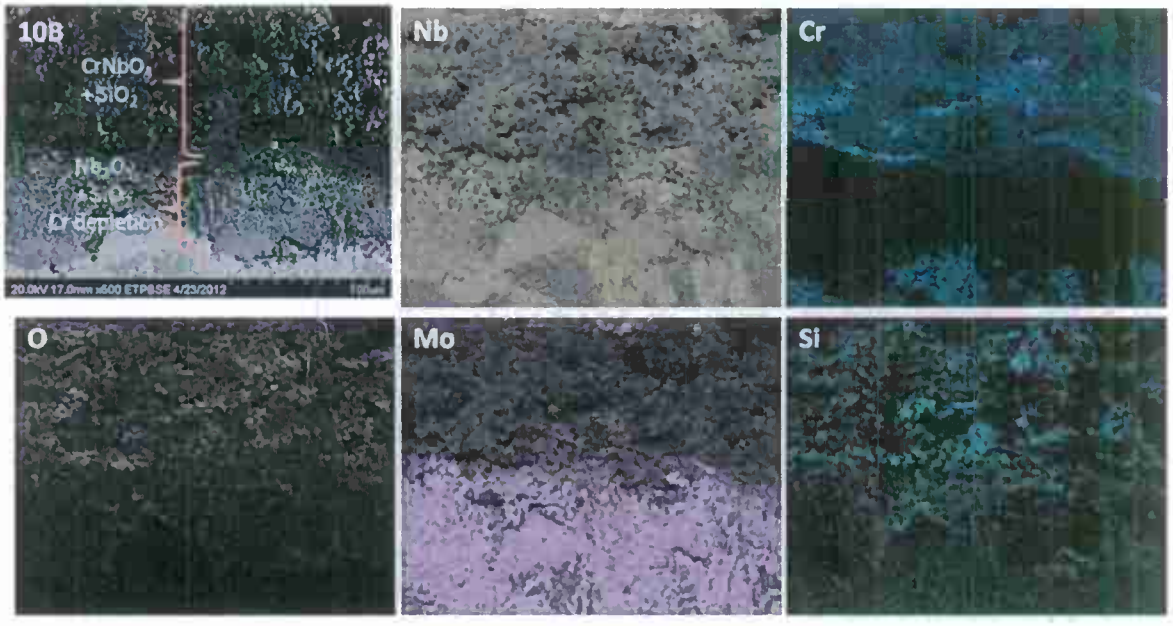

Figure 16. The x-ray mapping of the oxide-metal interface structure showing the elemental mapping for the elemental location.

The oxide-Metal interface structure for the 15B alloy is shown in Figure 17. The structure appears to be almost identical to the features shown in Figure 15. The scale mainly consists of CrNbO4 and Nb2O5 while the IOL contains Cr depletion and Mo enrichment regions. The IOL seems to be much denser. It has the advantage of providing better oxidation resistance because it renders the permeability of oxygen through it to reach the alloy for further oxidation more difficult. Corresponding x-ray mapping (Figure 17) ensures the elemental locations of from the oxides. XRD results in conjunction with EDS and x-ray mapping does allow the identification of the oxides with more confidence and reliable. X-ray mapping for Si at 1300°C for 15B alloy shows that SiO2 is in immediate contact with the alloy indicating the preferential oxidation silicides in the substrate. Once again Cr depleted region is vividly shown in the Cr map. The Nb and Mo maps shows similar locations meaning that there is, perhaps, a mixture of oxides of Mo and Nb_2O_5 coexist in the structure. It must be noted that Nb_2O_5 and SiO_2 form the basis for IOL along with Cr depletion. Not only the IOL is dense even the rest of the scale is also dense in 15B alloy. All these microstructural features attest to the claim of this PI that 15B alloy provides best oxidation resistance for a Nb alloy thus far.

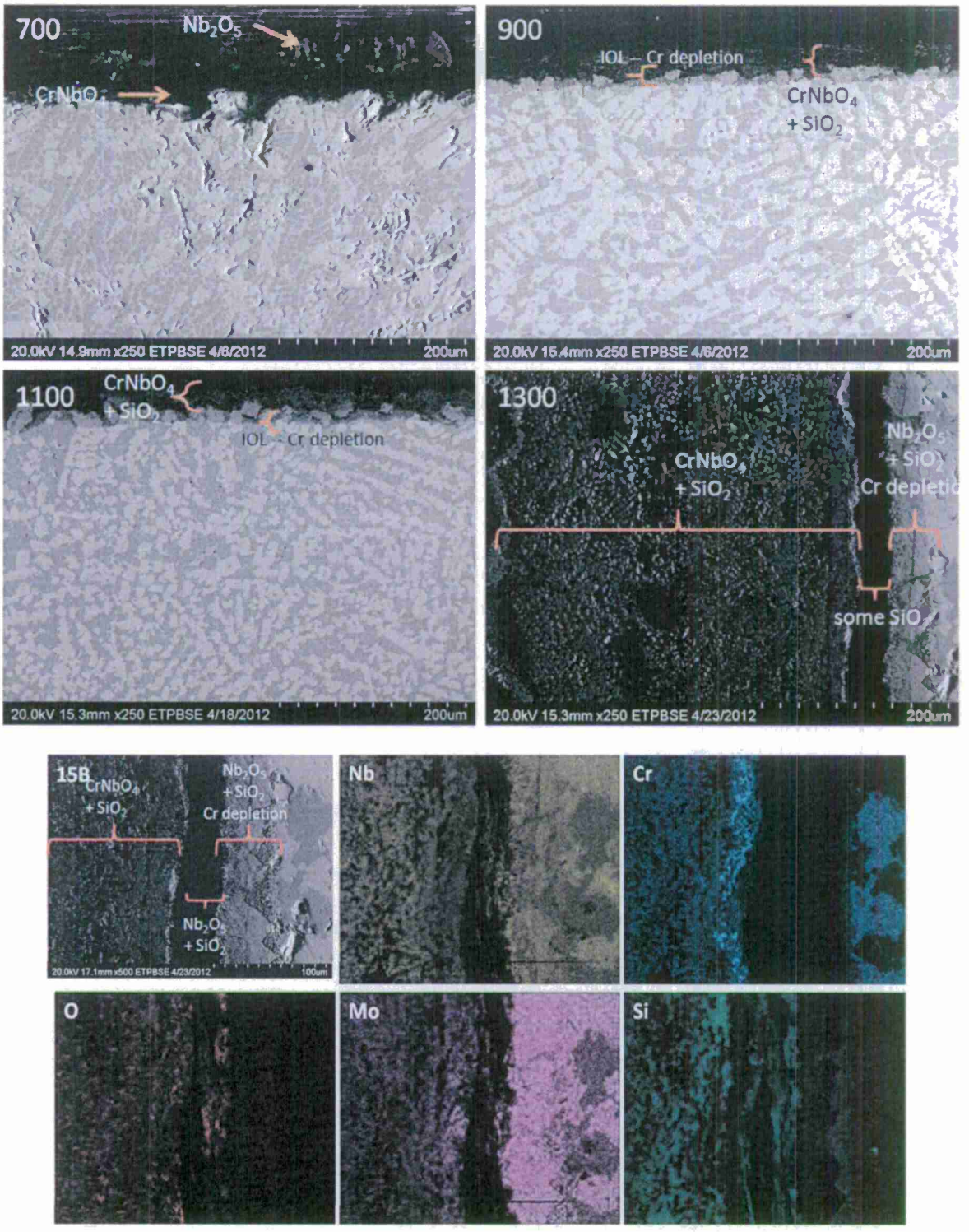

Figure 17. Oxide-Metal interface microstructure for 15B alloy after 3 day static oxidation in air at 700, 900, 1100, and 1300°C. The lower part shows the x-ray mapping for the elemental location of 15B alloy at 1300°C.

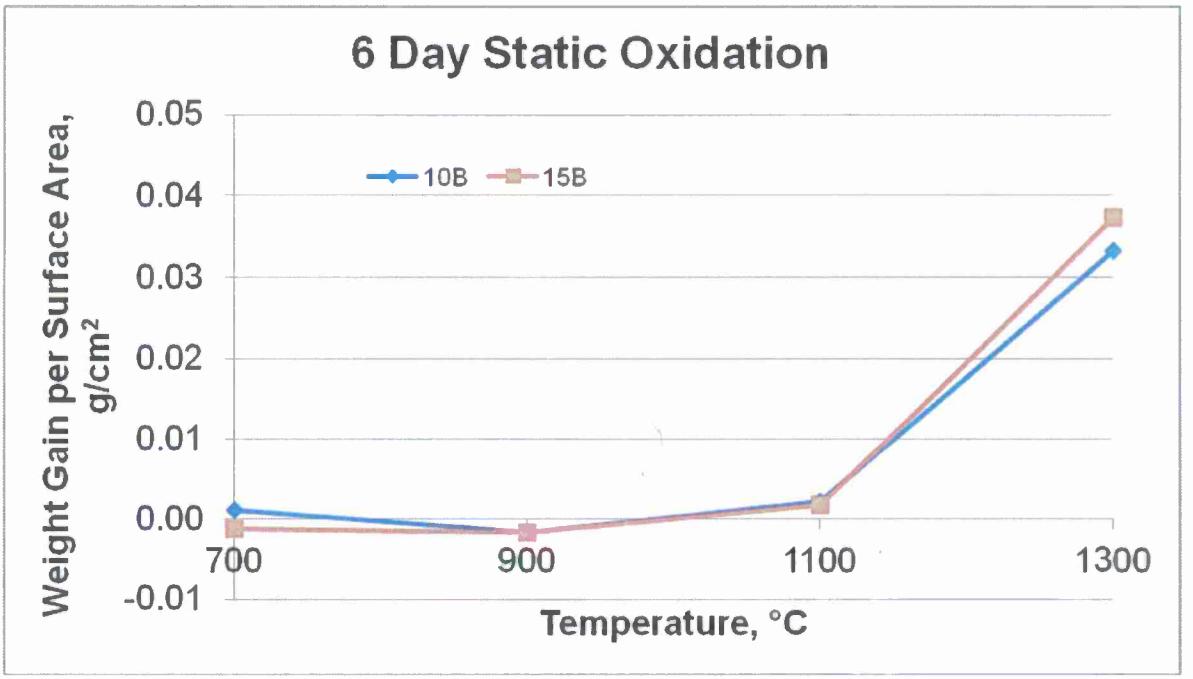

Figure 18. A comparison of the 6 day static oxidation curves between 10B and 15B alloy at 700, 900, 1100 and 1300°C.

A comparison of the 6 day static oxidation curves for 10B and 15B alloys is shown in Figure 18. The figure indicates virtually no change in the oxidation behavior of the two alloys surprisingly in this temperature range. In fact the weight gain per unit area values at 900 and 1100°C are identical. However, the value is smaller at 1300°C for 15B but it is considered as an experimental scatter rather than an actual trend.

A comparison between the cyclic and static oxidation behavior for 6 days of heating can be seen in Figure 19. Static oxidation for 10B alloy consistently shows higher weight gain per unit value than the corresponding values for cyclic oxidation. However, the curves for 15B alloy do not allow the similar comparison to be made. On the other hand, static oxidation shows lower value compared to cyclic oxidation for this alloy. Based on the trends indicated by the curves in Figure 19 no definite conclusion can be made regarding a comparison between the two different modes of heating involved for oxidation. It must be noted, though, that the heating at the oxidation temperature is more than cyclic mode. It can be thus stated that either this study cannot make such a distinction or it does not make a difference in these two types of modes of heating for these two alloys even up to a temperature of 1300°C.

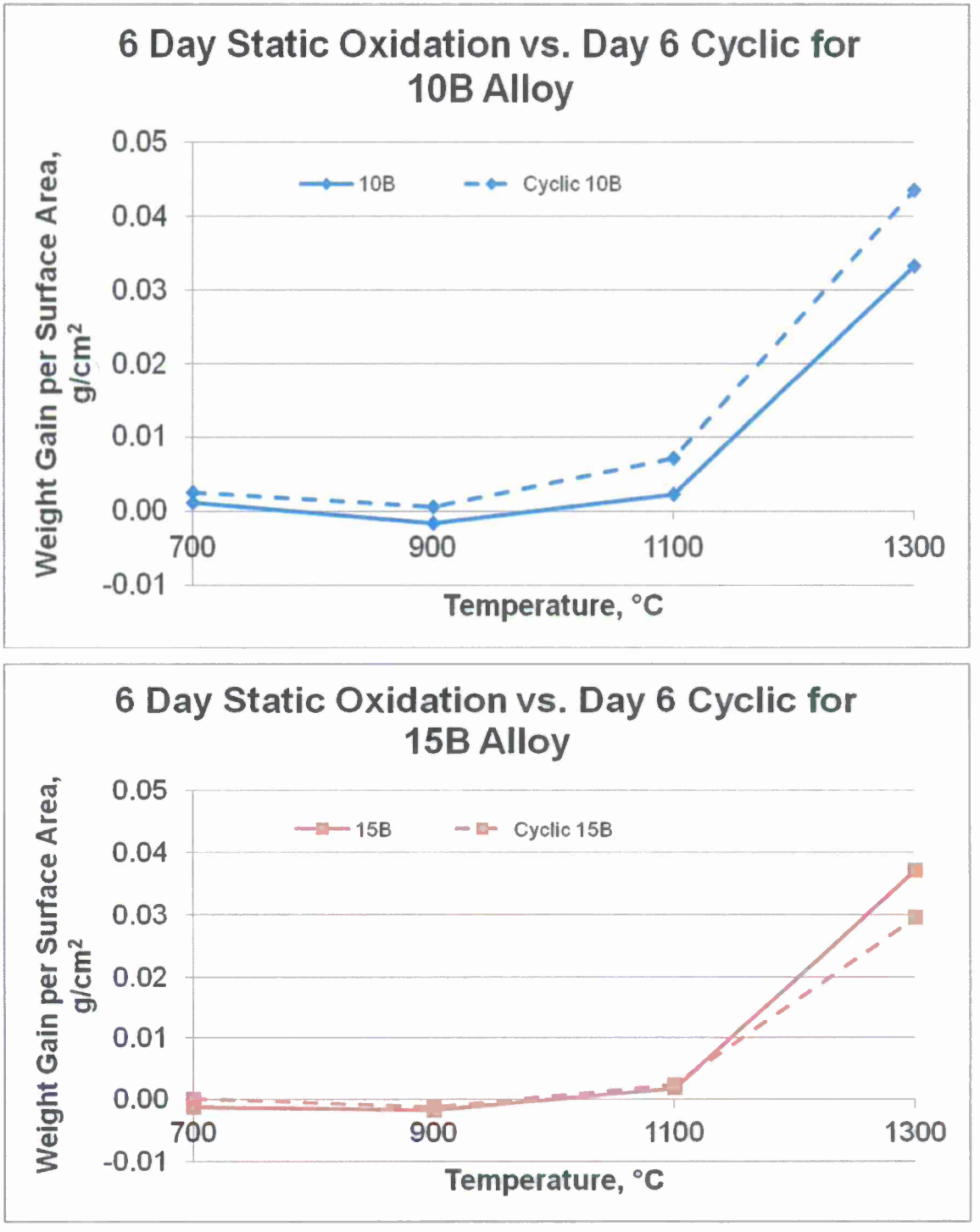

Figure 19. A comparison of static and cyclic oxidation curves for 10B and 15B alloys.

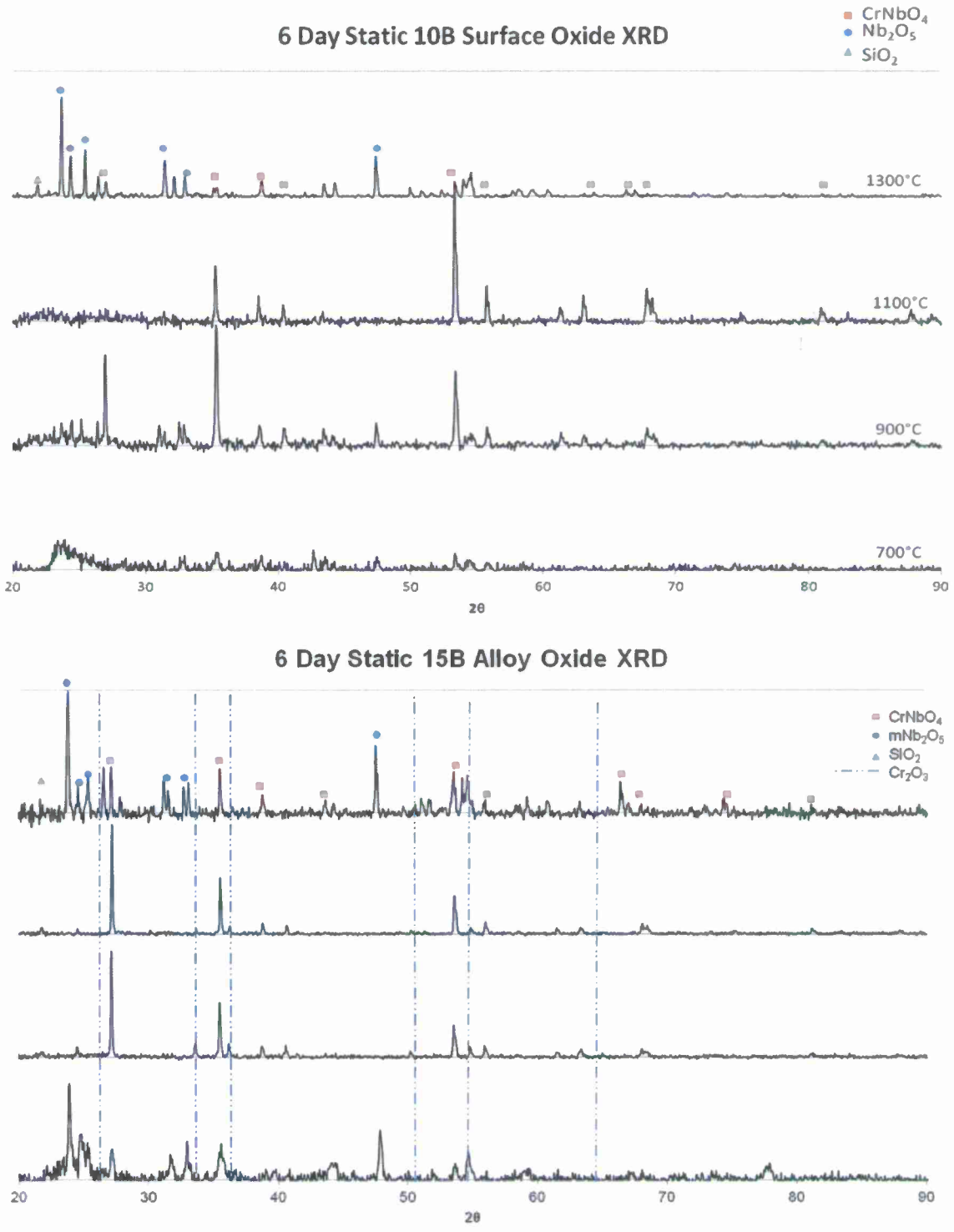

Figure 20. XRD patterns of the oxidation products for 10B and 15B alloys after heating for 6 days under static oxidation mode.

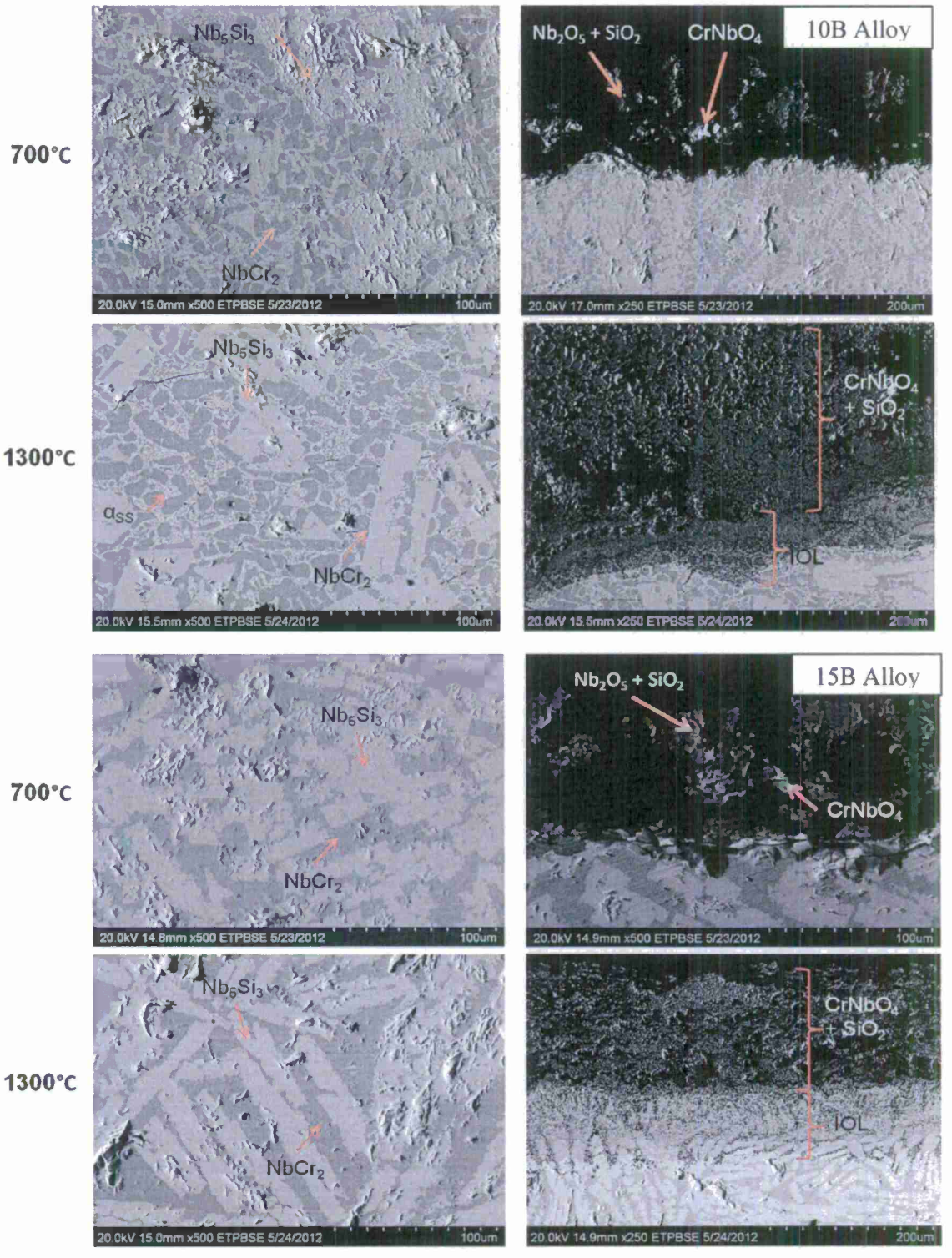

Figure 21. Microstructures of the matrices and oxide-metal interface for 10B and 15B alloys at 700 and 1300°C after 6 days of static oxidation.

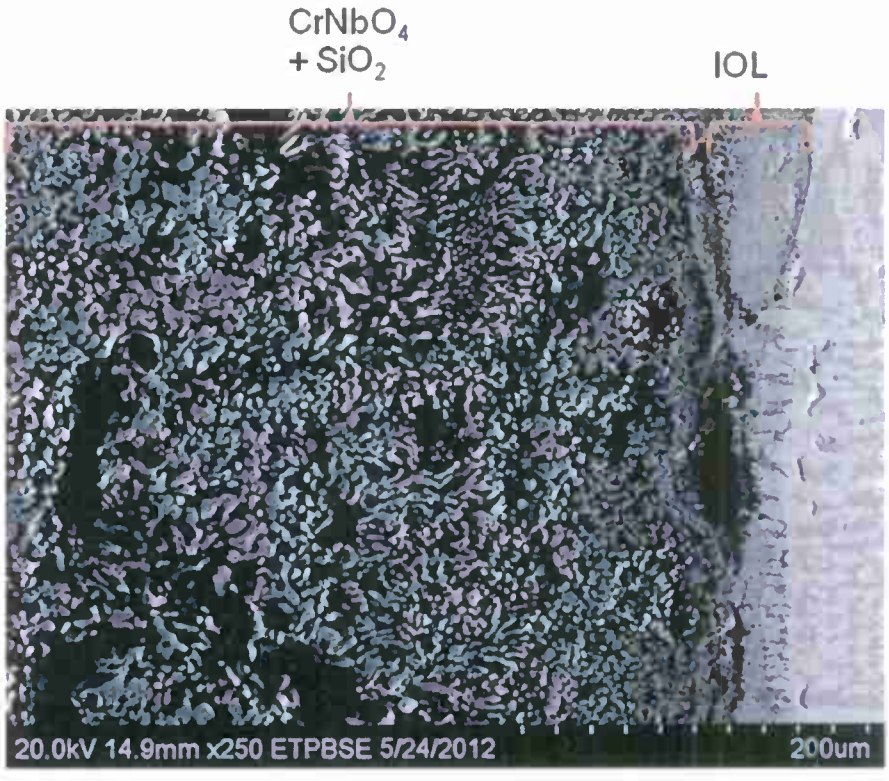

Figure 22. Details of oxide-metal interface for 15B alloy at 1300oC for 6 day heating under static oxidation mode.

Nb-Cr-Si System

Nb-Cr-Si system was studied to determine the combined influence of Cr and Si on the oxidation resistance of alloys from this system in general. The precious study from this research indicated that no beneficial effects were produced by exceeding the Cr concentration to beyond 25 atomic percent. So it was decided to keep the Cr concentration to 20 atomic percent but vary the Si from 10 to 42 at%. The specific alloys studied had a nominal compositions of Nb-20Cr-10Si, Nb-20Cr-20Si, Nb-20Cr-30Si, and Nb-20Cr-42Si.

It is well known that the oxidation resistance of alloys from Nb-Cr-Si system is strongly dependent on the microconstituents in the microstructures. The two main phases consist of Nb_5Si_3 and $NbCr_2$ (Laves phase). An isothermal section at room temperature (25°C) is shown in Figure 23.

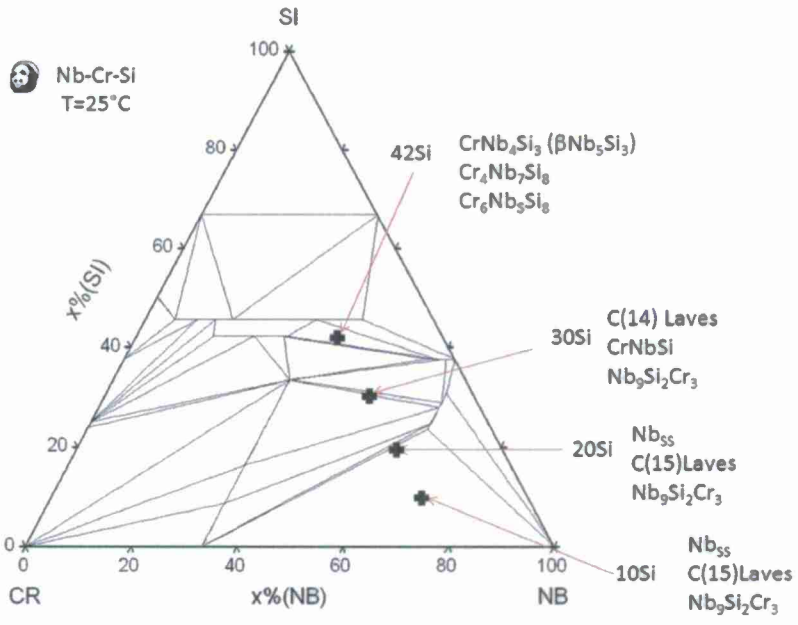

Figure 23. An isothermal section of Nb-Cr-Si phase diagram at 25°C.

An important observation from this section as calculated by a Pandat™ software shows the silicides can be expected in this system for the chosen composition. These silicides include Nb_5Si_3, $Nb_9Si_2Cr_3$, CrNbSi, $CrNb_4Si_3$, $Cr_4Nb_7Si_8$ and $Cr_6Nb_5Si_8$. The section also shows the phase like Nb_{ss} and two forms (at high and low temperature) of Laves phases. However the 10 and 20 Si alloys are expected to have identical typical microstructures with Nb_{ss}, $NbCr_2$ and

$Nb_9Si_2Cr_3$ phases. Nb_{ss} phase appears to be absent when the Si content is raised to 30% and the high temperature form of Laves phase (hexagonal C14 lattice) and CrNbSi and $Nb_9Si_2Cr_3$ are to be expected. It must be pointed out that C15 lattice form of Laves phase is known as low temperature form with a cubic lattice which appears for the 10 and Si alloys. The 42% alloy shows unique microstructure with $(Cr,Nb)11Si_8$ and $CrNb_4Si_3$ (a β form of Nb_5Si_3). The α and β forms of Nb_5Si_3 both have cubic structure. However, the β form is the high temperature form of this silicide unless stabilized.

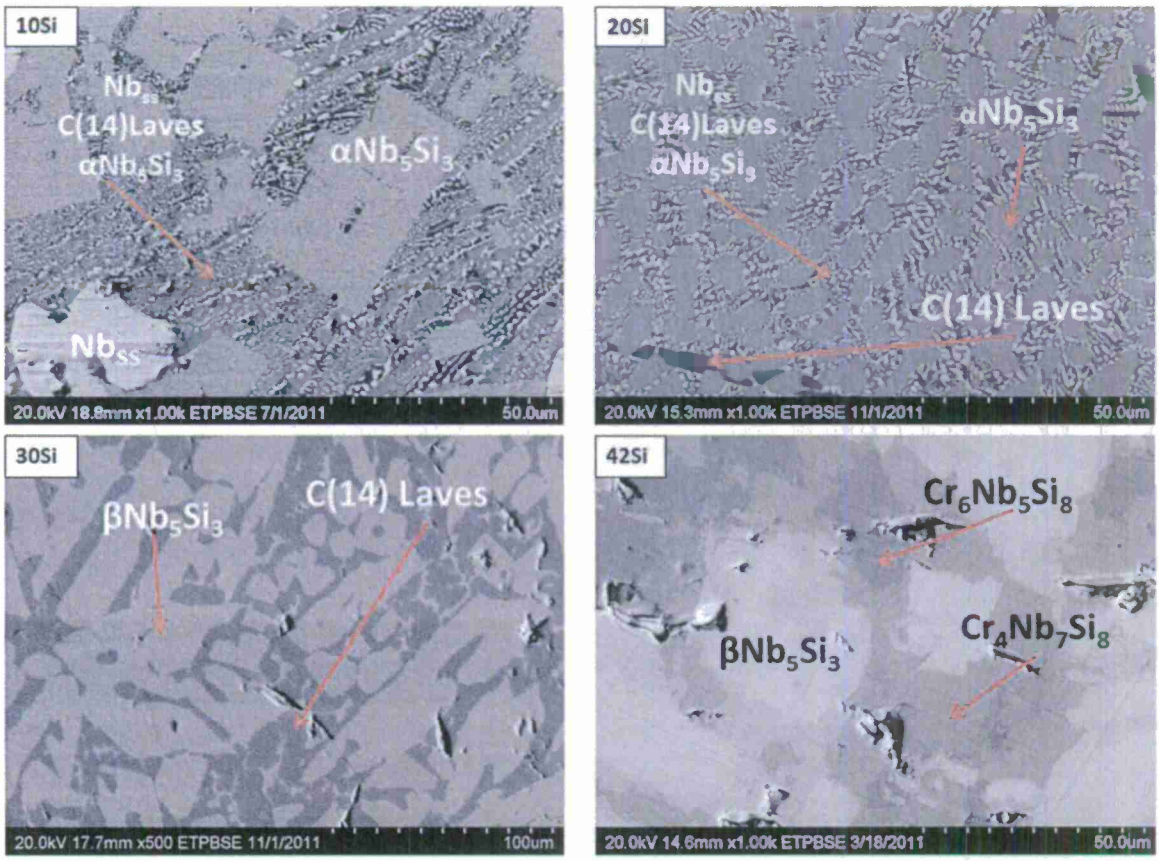

Figure 24. As-cast microstructures of 10, 20, 30 and 42Si alloys.

Figure 24 shows the as-cast microstructures of the four alloys studied in this phase of the research of this study.

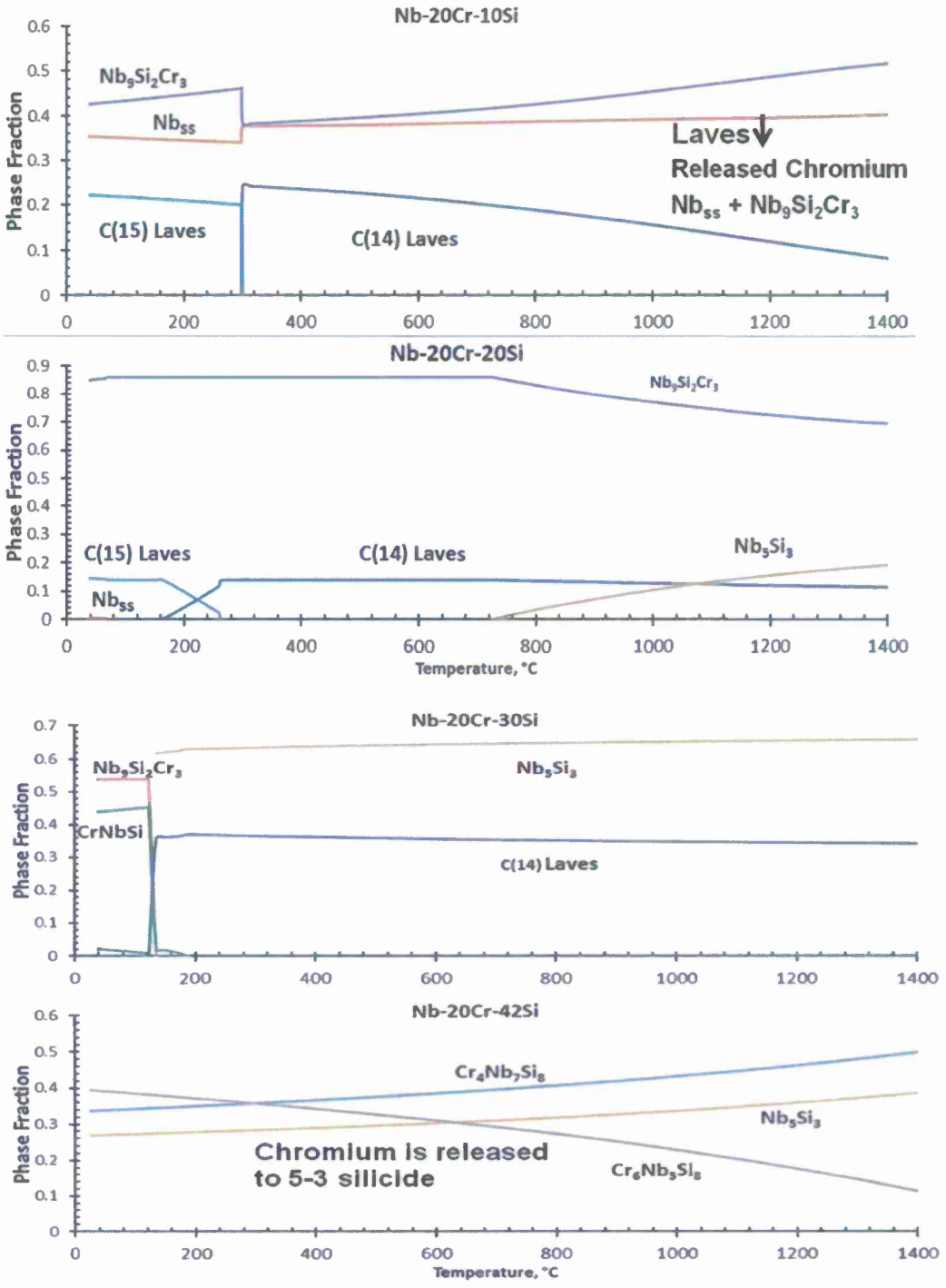

Figure 25. Phase fractions of phases as a function of transformation temperature.

Figure 25 shows the expected phase fractions as a function of transformation temperature for 10 and 20%Si alloys. The 10Si alloy shows that Nb_{ss} phase is stable only up to 300°C and the phase fraction rises slightly nearly 0.37 and then remains constant. Low temperature form of

Laves phase is to be expected only up to 300°C and high temperature phase fraction continually decreases from around 0.25 to less than 0.1 in a temperature range of 300 to 1400°C. The Cr released may be incorporated in to the increases phase fractions of $Nb_9Si_2Cr_3$ and Nb_{ss}. The increase in the amount of $Nb_9Si_2Cr_3$ from 300°C is significant. 20Si alloy, on the other hand, shows the dominance of only high temperature Laves and $Nb_9Si_2Cr_3$ phases while Nb_5Si_3 should begin to appear at slightly above 700°C and then rises sharply.

The phase fraction charts for 30 and 40Si alloys show that $Nb_9Si_2Cr_3$ phase does not appear at temperatures higher than 175°C while rather large phase fractions of Nb_5Si_3 and high temperatures phases are indicate for 30%Si alloy. The 42Si alloy begins to indicate the formation of new silicides not observed thus far in this study. It shows that $Cr_4Nb_7Si_8$ and Nb_5Si_3 phases both increase their amounts while $Cr_6Nb_5Si_8$ decreases with increase in temperature. This information also suggests that Cr released from $Cr_6Nb_5Si_8$ is involved in raising the Cr concentration in Nb_5Si_3.

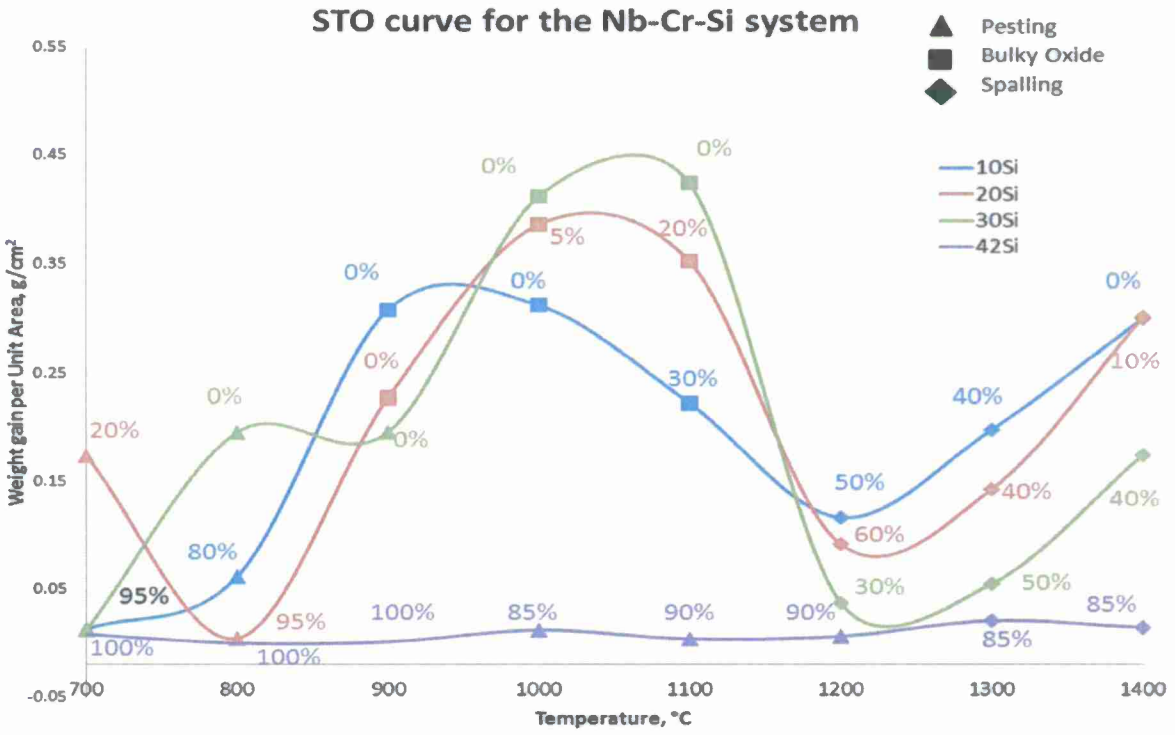

Figure 26. Oxidation curves for 10, 20, 30, and 42%Si alloys from 700 to 1400°C. The number indicate the amounts of metal left after oxidation treatment at each temperature

A graph (oxidation curves) between weight gain per unit area as a function of oxidation temperature is shown in Figure 26. It must be noted that the numbers on the curves show the amount of the metal left after oxidation at a given temperature for all the 4 alloys. The symbols show the dominance of the type of the oxidation type taking place at respective positions. The low temperature pesting problem associated with Nb alloys, in general, appears to be controlled at 700°C except for the 20%Si alloy. But the pesting problem with 30Si alloy worsens at 800 and 900°C while other 3 alloys have shown significant resistance for this type of oxidation. The major problem associated with Nb alloys of this study has been the formation of bulky oxide in the intermediate temperature range. This graph shows that this occurs at 900, 1000, and 1100°C except for the 42Si alloy. In fact, the amount of bulky oxide formation decreases with increase in Si content at 1100°C and then at higher temperatures spalling begins in all the alloys. At 1200 and 1300°C there is significant amount of metal left for all alloys regardless of the type of oxidation taking place. The exceptional behavior of 42Si alloy must be noted at 1400°C where 85% of the metal was retained. It shows remarkable oxidation resistance and is the best of all the various alloys for the ternary systems studied in this research. In fact, 42Si alloy demonstrate the excellent oxidation resistance in the entire temperature range of this study in terms of amount of metal left after the heating period.

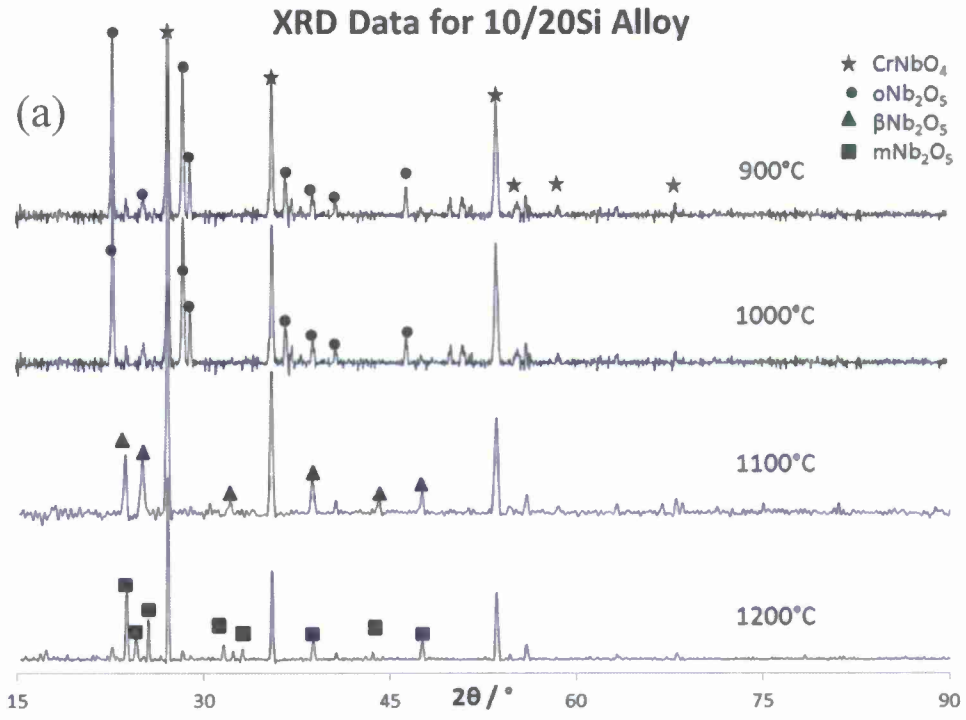

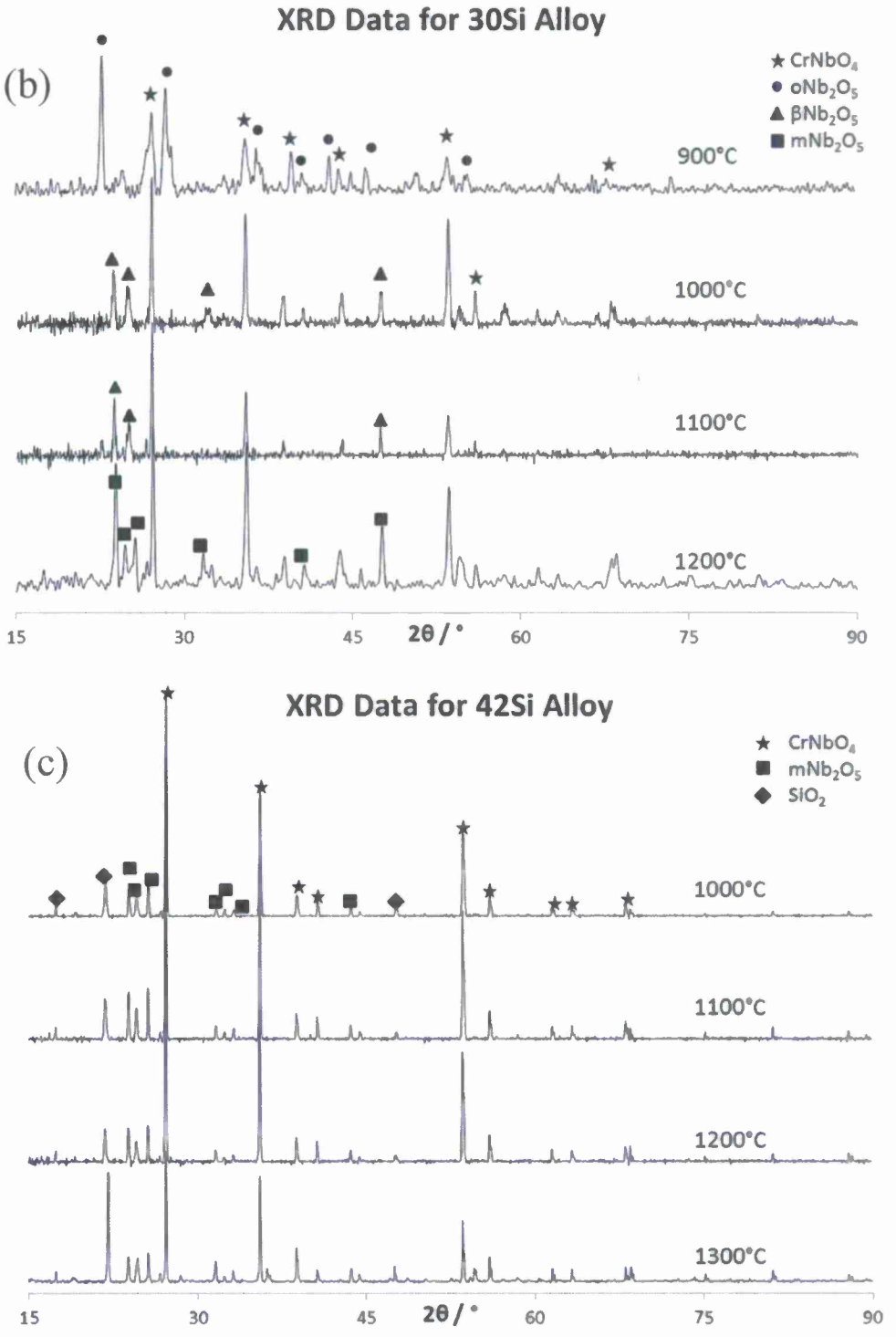

Figure 27. XRD patterns after oxidation for the 10/20, 30 and $42 Si alloys.

The XRD patterns shown in Figure 26 for 10/20Si alloys indicate the presence of βNb_2O_5 which has base centered monoclinic form is considered responsible for the formation of bulky oxide at the intermediate temperature range. The orthorhombic and monoclinic forms of Nb_2O_5 are present in the low and high temperature regimes. $CrNbO_4$ is present at all the oxidation temperatures of this study. It must be noted that this oxide is considered as desirable. The XRD patterns for 30 and 40Si alloys are nearly identical to those observed for 10/20Si alloys except for the subtle differences. For example, 30Si alloy shows both heavy pesting as well as bulky oxide formation except at 1200°C. 40Si alloy the best oxidation resistance and the XRD pattern for this alloy shows complete absence of base centered monoclinic form of Nb_2O_5. It appears that 40Si alloy inhibits the formation of this oxide and is responsible for the best oxidation resistance of the alloys from Nb-Cr-Si system studied thus far.

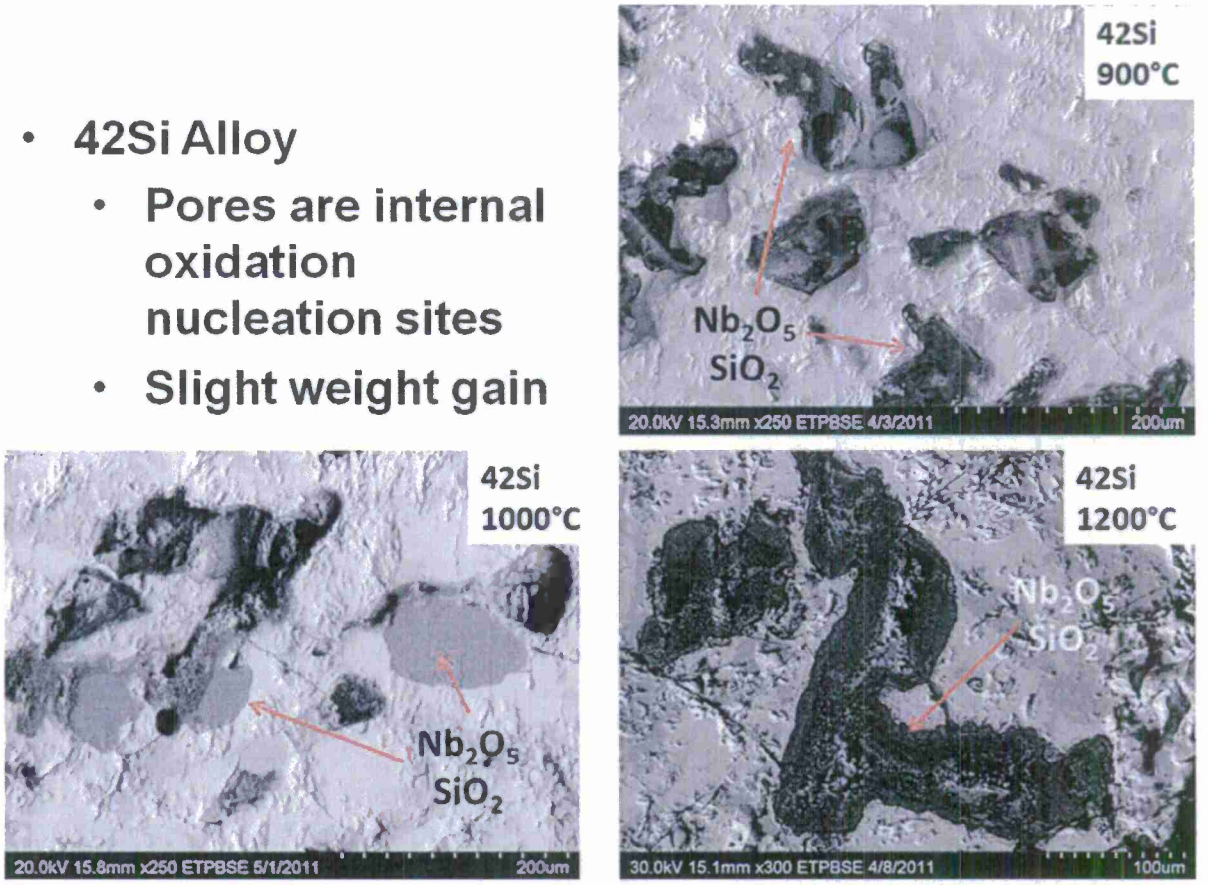

Figure 27 Oxidation features at the microscopic level for 42Si alloy.

The pores play an important role in the oxidation for 42Si alloy as these appears to act nucleation sites for oxidation. This nucleation of oxidation at internal pores is shown in Figure 27. Formation of Nb_2O_5 and SiO_2 are clearly marked in the micrographs. The lower right hand side micrograph indicates a perfect evidence to show that the oxidation can easily take place at the interior walls of the pores. Of course this type of oxidation also contributes to the overall oxidation but the overall effect seems to be least for the 4 alloys studied in this program.

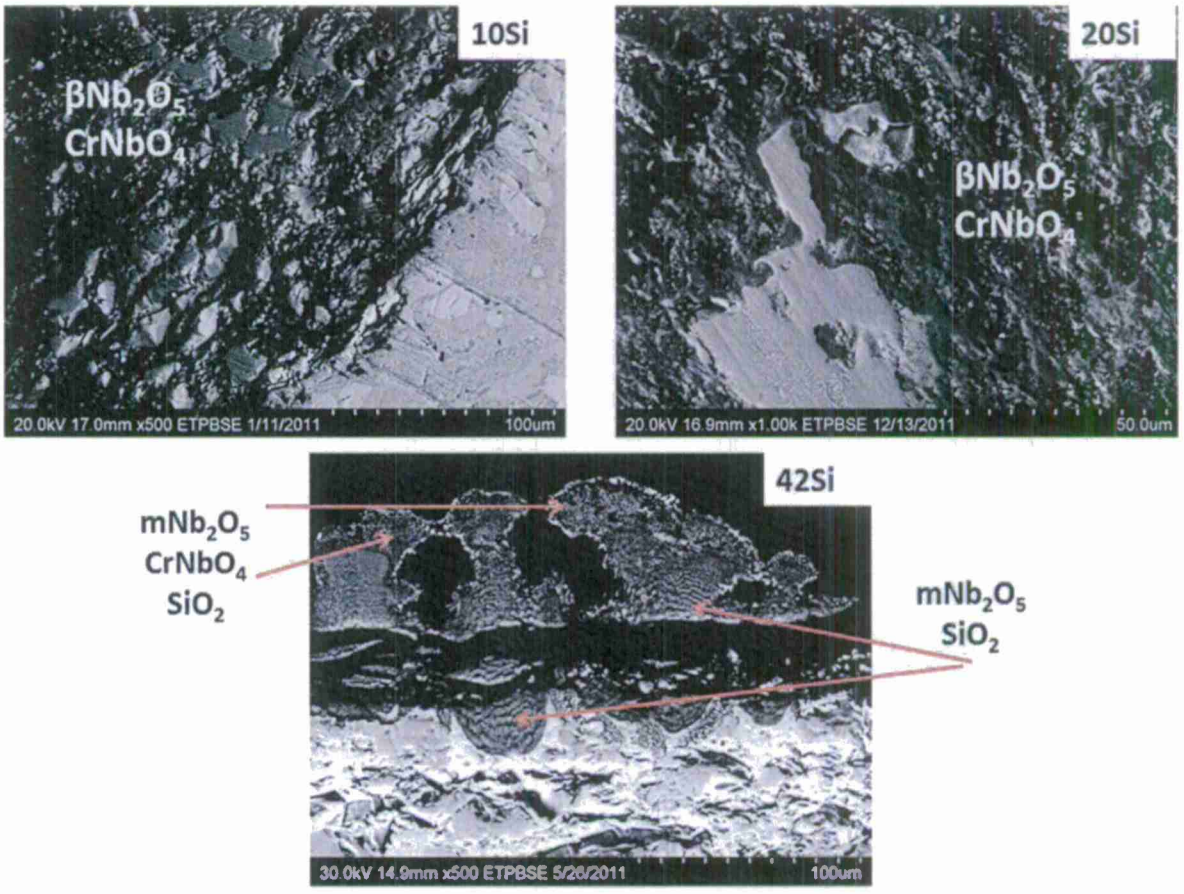

Figure 28 Comparison of the oxide-metal interface for the 10, 20 and 40Si alloys at 800°C.

Salient feature of this study is to indicate the presence of other forms of silicides formation besides Nb_5Si_3 which seem to affect the oxidation characteristics in 40Si alloy. $Cr_5Nb_6Si_8$ and $Cr_4Nb_7Si_8$ are the silicides that are present at this temperature as was discussed in reference to the ternary isothermal section. It was mentioned in reference to the as-cast microstructures. The phase fraction chart shows a continuous increase in $Cr_4Nb_7Si_8$ while $Cr_6Nb_5Si_8$ decreases with temperature. The decrease in $Cr_6Nb_5Si_8$ amount releases Cr which

appears to go in the Nb_5Si_3 in solution form which was mentioned before and was tested with EDS analysis. This βNb_5Si_3 is the Cr enriched form of normal Nb_5Si_3. It is speculated that this microstructural feature is responsible for almost absence of any oxide scale in this scale as

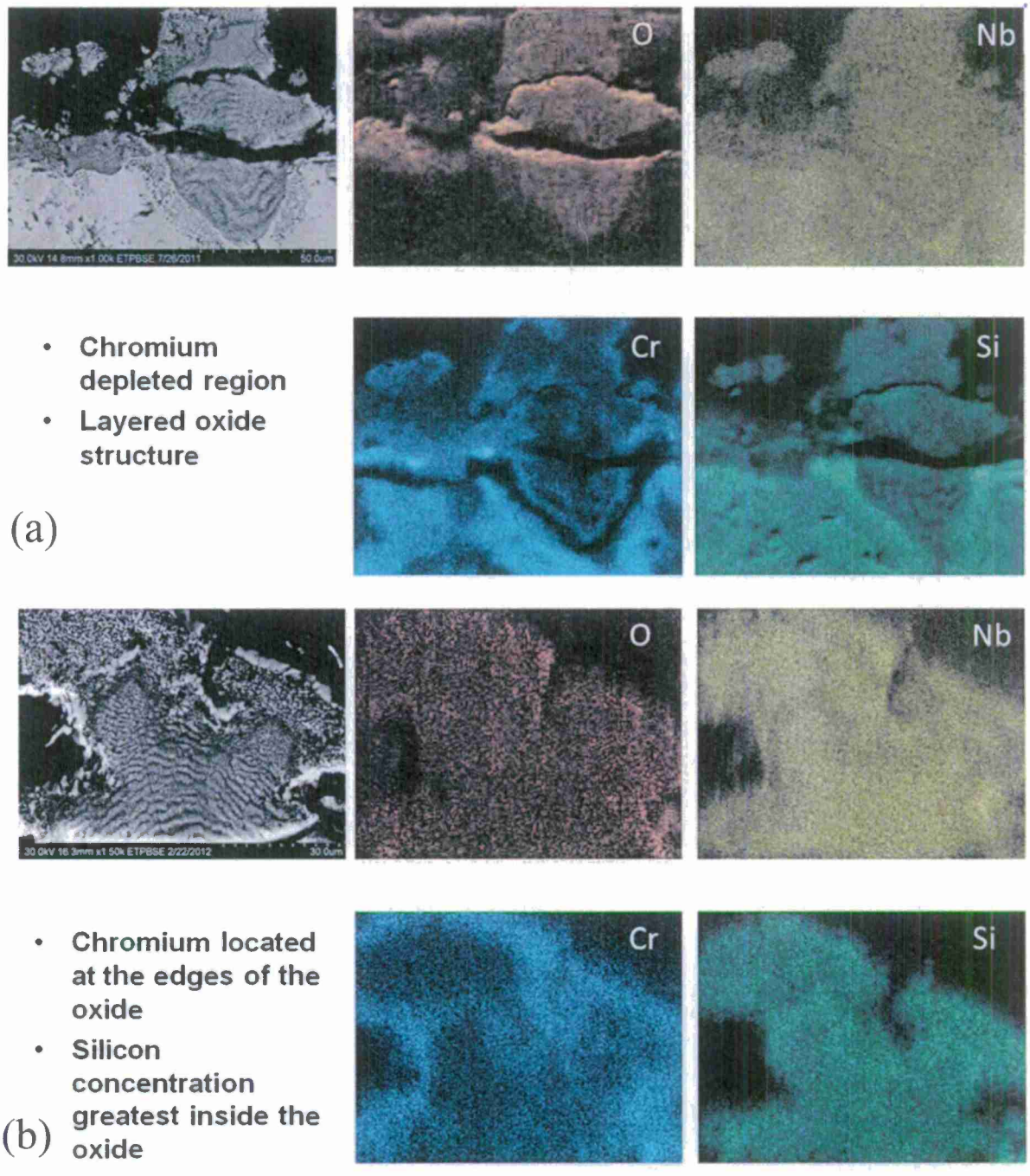

Figure 29 Elemental distribution at the metal-interface resolved at (a) low and (b) high magnifications at 1100°C.

shown in Figure 28.

Figure 29 shows the elemental distribution at the metal interface for the 42Si alloy at 1100°C. The purpose of Figure 29(a) is a lower magnification picture showing the overall elemental distribution. The little trough shown shows the layered oxidized region consisting of alternate layers of Nb_2O_5 (light) and SiO_2 (dark). This area is immediately surrounded by a thin Nb_2O_5 layer and then SiO_2 enriched region. However this is exactly on the metal surface which is separated from the oxide scale by a certain amount of void space. Bright spots for Si representing SiO_2 must be noticed. The SiO_2 black dots are surrounded by Cr rich area. Cr enriched area zone can be easily recognized by the higher magnification shot shown in Figure 29(b). The bright area in the BSE mode is the Cr enriched with $CrNbO_4$ outlines the patch while rest is shown as Si rich containing SiO_2 and Nb rich with Nb_2O_5. However, the alternate layers are not well resolved in either parts of this figure.

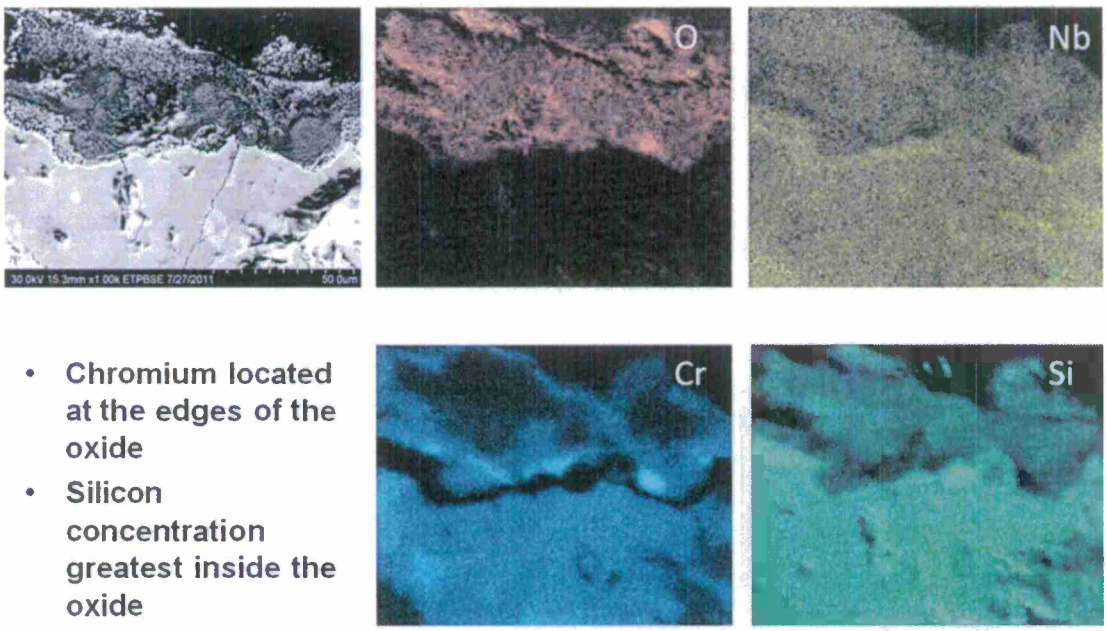

Figure 30 Elemental distributions at the metal-oxide interface for 42Si alloy at 1200°C.

The respective formation of Nb_2O_5, SiO_2, $CrNbO_4$ at the metal oxide interface continues after oxidation at 1200°C. The initiation of oxidation process was studied by an experiment for 15 minute heating period at 900, 1100 and 1300°C in air. The oxide layer can be barely recognized at 900oC while it is noticeable at 1100oC as shown in Figure 31. Oxidation is initiated by the simultaneous formation of SiO2 and Nb2O5 at the metal interface while the separations between the oxide scale and metal surface due to uneven CTE values for the various

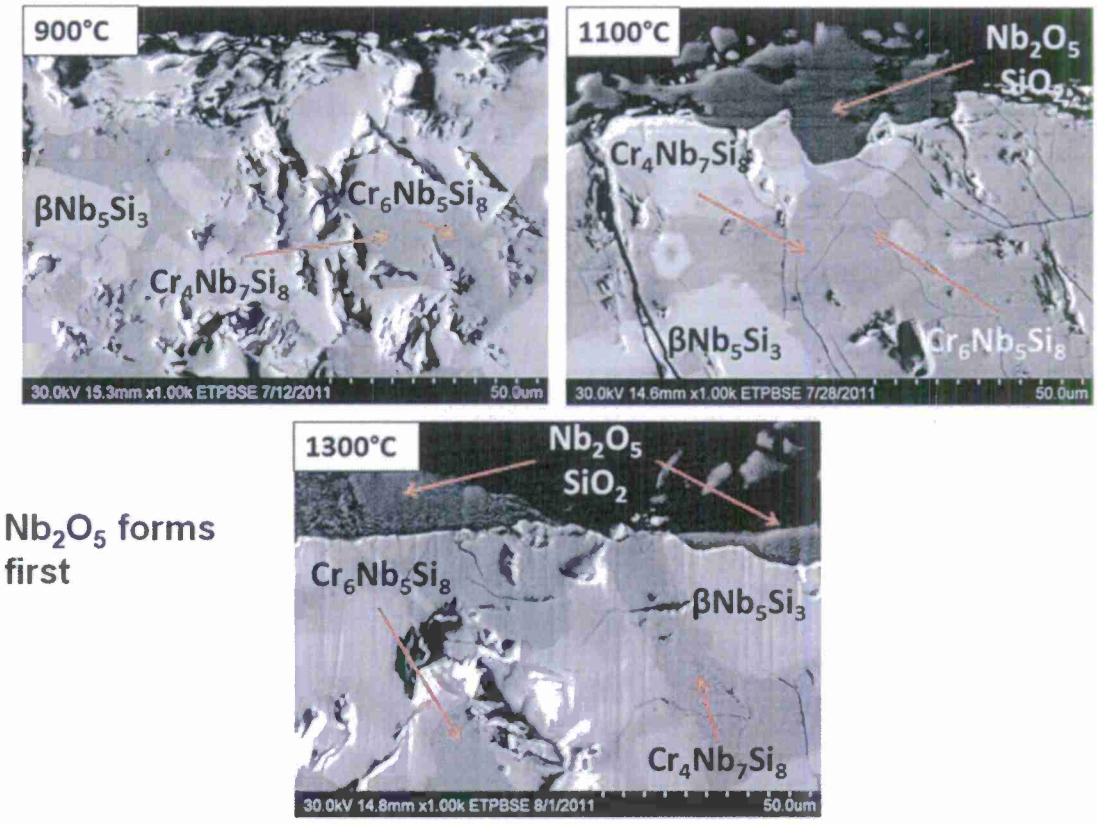

Figure 31 Microstructural evolution for the oxidation process for 42Si alloy for a 15 minute experiment at 900, 1100, and 1300°C.

oxides and the metal have not been observed for 15 minute oxidation. Continued and rapid, relatively speaking, oxidation can be seen at 1300°C.

Publications

1. "Oxidation Resistance of Nb-20Mo-15Si-5B-20Cr up to 1,300°C"
   Julieta Ventura and S.K. Varma
   Journal of Metals
   Vol.61, 72-75, 2009

2. "Oxidation Resistant $NbCr_2$ Phase in Nb-W-Cr System"
   Julieta Ventura, Benedict Portillo, and S.K. Varma
   Journal of Alloys and Compounds
   Vol.476, 257-262, 2009 (doi:10.1016/j.jallcom.2008.09.164)

3. "Oxidation Behavior of Nb-20Mo-15Si-5B-20Cr and Nb-20Mo-15Si-5B-20Ti Alloys Up To 1300°C"
   Julieta A. Ventura, Benedict I. Portillo, Shailendra K. Varma, and Rabindra N. Mahapatra
   ECS Transactions (doi: 10.1149/1.3224752@The Electrochemical Society)
   Vol.16, Issue 44, pp.157-166, 2009

4. "Heat Treatment and Oxidation Characteristics of Nb-20Mo-15Si-5B-20(Cr,Ti) Alloys from 700 to 1400°C"
   Sylvia Natividad, Arianna Acosta, Krista Amato, Julieta Ventura, Benedict Portillo, and S.K. Varma
   Materials Science Forum
   Vols. 638-642, 2351-2356, 2010 (doi:10.4028/www.scientific. net/MSF.638-642.2351)

5. "Oxidation behavior of Nb-20M0-15Si-5B-20Ti Alloy in Air from 700 to 1300°C"
   Benedict Portillo and S.K. Varma
   Journal of Alloys and Compounds
   Vol. 497, 68-73, 2010 (doi:10.1016/j.jallcom.2010.03.005)

6. "Microstructures and High Temperature Oxidation Resistance of Alloys from Nb-Cr-Si System"
   S.K. Varma, Clemente Parga, Krista Amato, Jennifer Hernandez
   Journal of Materials Science
   Vol. 45, 3931-3937, 2010 (doi: 10.1007/s10853-010-4458-8)

7. "High Temperature Alloys from Nb-Cr-Si System with Minor Additions"
   Benedict Portillo, David Alvarez, and Alma Vazquez, Shailendra K. Varma
   Materials Science Forum

Vols. 654-656, 570-573, 2010 (doi:10.4028/www.scientific. net/MSF.654-656.570)

8. "Oxidation of Nb-Cr-Si Alloys at Temperatures Above 1000°C"
S.K. Varma, Benedict Portillo, David Alvarez, and Alma Vazquez
World Journal of Engineering
Supplement 2, 442-443, 2010

9. "Characterization of Microstructures and Oxidation Behavior of Nb-20Si-20Cr-5Al Alloy"
David Alvarez and S.K. Varma
Corrosion Science
Vol.53, 2161-2167, 2011 (doi:10.1016/j.corsci.2011.02.038)

10. "High Temperature Oxidation Behavior of Nb-Cr-Si Alloys with Hf Additions"
Alma Vasquez and S.K. Varma
Journal of Alloys and Compounds
Vol.509, 7027-7033, 2011 (doi: 10.1016/j.jallcom.2011.02.174)

11. "Effect of Cr on the Oxidation Resistance of Nb-Cr-Mo-Si-B Alloy"
S.K. Varma and Benedict Portillo
World Journal of Engineering
Supplement 1, 1151-1152, 2011

12. "Oxidation Behavior of Nb-20Mo-15Si-25Cr and Nb-20Mo-15Si-25Cr-5B Alloys"
Benedict I. Portillo and S.K. Varma
Metallurgical and Materials Transactions A
Vol.43, 147-154, 2012 (doi: 10.1007/s11661-011-0861-2)

13. "The effects of uncommon silicides on the oxidation behavior of alloys from the Nb-Cr-Si system"
D. Brendan Vogelwede and S.K. Varma
Corrosion Science
Vol.61, 123-133, 2012 http://dx.doi.org/10.1016/j.corsci.2012.04.029

14. "A Comparison of the Effect of Cr and Al additions on the Oxidation Behavior of Alloys from the Nb-Cr-Si System"
Nydia Esparza, Victoria Rangel, Amanda Gutierrez, Brenda Arellano, and S.K. Varma
Materials at High Temperatures
Submitted for publication

Presentations

1. "Oxidation Behavior of Nb-15Si-20Mo-5B-20Ti Alloys Between 700 and 1300°C"
   Benedict Portillo, Shailendra Varma, Julieta Ventura, and Rabindra Mahapatra
   Symposium on ***Materials for High Temperature Applications***: The Next Generation Superalloys and Beyond: Refractory Metals I
   138th Annual Meeting and Exhibition, TMS 2009
   San Francisco, CA, February 17, 2009

2. Microstructural Development of Nb-15Si-20Mo-5B-20Ti and Nb-15Si-20Mo-5B-20Cr Alloys in Air and Argon Atmospheres from 600 to 1300°C"
   Benedict Portillo, S.K. Varma, and R. Mahapatra
   215th ECS Meeting #653
   San Francisco, California, May 26, 2009.

3. "Heat Treatment and Oxidation Characteristics of Nb-20Mo-15Si-5B-20(Cr,Ti) Alloys from 700 to 1400°C"
   S.K. Varma, Sylvia Natividad, Arianna Acosta, Julieta Ventura, Benedict Portillo
   Symposium on ***Heat Treatment of Steels & Superalloys I***
   THERMEC'2009, International Conference on Processing & Manufacturing of Advanced Materials, Processing, Fabrication, Properties, Applications
   Berlin. Germany, August 28, 2009

4. "Oxidation Behavior of Alloys from Nb-Cr-Si System from 700 to 1300°C"
   S.K. Varma
   Symposium on ***High Temperature Corrosion and Materials Chemistry***: Fundamentals of Alloy oxidation, II
   216th ECS Meeting. #1842
   Vienna, Austria, October 7, 2009

5. "Oxidation Behavior of Nb-30Si-10Cr and Nb-30Si-20Cr up to 1400°C"
   Clemente Parga, Benedict Portillo, and Shailendra Varma
   Symposium on ***Environmental Degradation and Protection of High Temperature Alloys***
   MS&T'09, TMS Fall Meeting
   Pittsburgh, Pennsylvania, October 26, 2009

6. "A Comparison of Theoretically Calculated and Experimentally Observed Microstructures in Alloys from Nb-Cr-Si System"

Sylvia Natividad, Krista Amato, Arianna Acosta, Kimberline Schnittker, Jennifer Hernandez, David Alvarez, and Shailendra Varma
Symposium on ***Environmental Degradation and Protection of High Temperature Alloys***
MS&T'09, TMS Fall Meeting
Pittsburgh, Pennsylvania, October 27, 2009

7. "Comparison of the Oxidation Behavior of Nb-20Mo-15Si-25Cr and Nb-20Mo-15Si-25Cr-5B Alloys from 700 to 1300°C"
Benedict I Portillo and Shailendra K. Varma
Symposium on ***Refractory Metals 2010***
139th Annual Meeting and Exhibition, TMS 2010
Seattle, Washington, February 16, 2010

8. "Effect of Al on the Oxidation Behavior of Nb-Si-Cr Alloys in Air from 700 to 1300°C"
Clemente Parga, David Alvarez, and Shailendra Varma
Symposium on ***Refractory Metals 2010***
139th Annual Meeting and Exhibition, TMS 2010
Seattle, Washington, February 16, 2010

9. "Influence of Al and Hf Addition on the Oxidation Resistance of Nb-20Si-20Cr-5(Al, Hf) Alloys"
A. Vasquez, D. Alvarez and S. Varma
217th ECS Meeting, Abstract # 877
Vancouver, Canada, April 28, 2010

10. "Oxidation of Nb-Cr-Si Alloys at Temperatures Above 1000°C"
S.K. Varma, Benedict Portillio, David Alvarez, and Alma Vazquez
18th International Conference on Composites or Nano Engineering
Anchorage, Alaska, July 4-10, 2010

11. "High Temperature Alloys from Nb-Cr-Si System with other Minor additions"
Shailendra Varma; Benedict Portillo; David Alvarez; Alma Vazquez
The 7th Pacific Rim International Conference on Advanced Materials and Processing (PRICM 7)
Cairns, Australia, August 1-5, 2010

12. "Oxidation Behavior of Nb-20Si-20Cr Alloy with Hf Additions"
Alma Vazquez, Krista Amato, Shailendra Varma
Symposium on Dr. John J. Stephens, Jr. Memorial Symposium: Deformation and Interfacial Phenomena in Advanced High-temperature Materials

Materials Science & Technology 2010
Houston, Texas, October 20, 2010

13. "Effect of the Cr, Si and B on the Oxidation Behavior of three Nb-base Alloys"
David Alvarez, Jennifer Hernandez, Shailendra Varma
Symposium on Dr. John J. Stephens, Jr. Memorial Symposium: Deformation and Interfacial Phenomena in Advanced High-temperature Materials
Materials Science & Technology 2010
Houston, Texas, 20, 2010

14. "Changes in Microstructures from 700 to 1400°C in Nb-Cr-Si-(5, 10)Hf Alloys"
Poster Session Only
Krista Amato, John Polkowske, Brenda Arellano, Alma Vazquez, Shailendra Varma
Symposium on Dr. John J. Stephens, Jr. Memorial Symposium: Deformation and Interfacial Phenomena in Advanced High-temperature Materials
Materials Science & Technology 2010
Houston, Texas, October 17-21, 2010

15. "Phase Stability in Nb-(20,25)Cr-(20,15)Si-5Al Alloys from 700 to 1400°C"
Poster Session Only
Jennifer Hernandez, Katherine Thomas, Eduardo Soto, David Alvarez, Shailendra Varma
Symposium on Dr. John J. Stephens, Jr. Memorial Symposium: Deformation and Interfacial Phenomena in Advanced High-temperature Materials
Materials Science & Technology 2010
Houston, Texas, October 17-21, 2010

16. "High Temperature Oxidation Resistance a Nb-20Si20Cr-5Al Alloy"
S.K. Varma
Processing and Fabrication of Advanced Materials (PFAM-19)
Auckland, New Zealand, January 14-17, 2011

17. "Oxidation Behavior of Nb-25Cr-20Si-15Mo-5B and Nb-25Cr-20Mo-15Si-10B in air from 700 to 1300°C"
Benedict Portillio and S.K. Varma
2011 TMS Annual Meeting &Exhibition
Refractory Metals 2011
San Diego, California, February 27 – March 3, 2011.

18. "Effect of Cr on the Oxidation Resistance of Nb-Cr-Mo-Si-B Alloys"
S.K. Varma

19th Annual International Conference on Composites, Nano or Metal Engineering ICCE-19
Shanghai, China, July 24-30, 2011.

19. "Effect of Al on the Oxidation Resistance of Alloys from Nb-Si-Cr System"
Nydia Esparza and Shailendra Varma
Refractory Materials
Advanced Protective Coatings for Refractory Metals and Alloys
Columbus, Ohio, October 16-20, 2011

20. "Oxidation Resistance of Nb Based Alloys from 700 to 1400°C"
Invited Paper
Shailendra Varma
Refractory Materials
Advanced Protective Coatings for Refractory Metals and Alloys
Columbus, Ohio, October 16-20, 2011

21. "Characterization of the Oxidation Behavior of Nb-20Si-20Cr Alloy"
Shailendra Varma and Daniel Voglewede
Poster
Refractory Materials
Advanced Protective Coatings for Refractory Metals and Alloys
Columbus, Ohio, October 16-20, 2011

22. "Oxide Scale Development in Select Alloys from the Nb-Mo-Cr-Si-B System"
Shailendra Varma, Eduardo Soto, Katherine Thomas, and Benedict Portillo
Poster
Refractory Materials
Advanced Protective Coatings for Refractory Metals and Alloys
Columbus, Ohio, October 16-20, 2011

23. "Comparison of Oxidation Behavior of Nb-20Si-20Cr-5Hf and Nb-20Si-20Cr-5Al Alloys"
Poster
Shailendra Varma, Brenda Arellano, Amanda Gutierrez, Alma Vasquez and David Alvarez
Refractory Materials
Advanced Protective Coatings for Refractory Metals and Alloys
Columbus, Ohio, October 16-20, 2011

24. "Oxidation Behavior of Nb-10Si-20Cr and Nb-10Si-20Cr-5Al Systems"
Victoria Rae Rangel and S.K. Varma
Refractory Metals 2012
Orlando, Florida, March 14, 2012

25. "The Effects of Silicon on the Nb-Cr-Si System"
Daniel Brendan Voglewede and S.K. Varma
Refractory Metals 2012
Orlando, Florida, March 14, 2012

26. "Effect of Al on the Oxidation behavior of Alloys from Nb-Cr-Si System"
Poster
Amanda P. Gutierrez and S.K. Varma
Refractory Metals 2012
Orlando, Florida, March 14, 2012

27. "B Addition to Nb-25Cr-20Mo-15Si Alloy for oxidation Resistance Up To 1400°C"
S.K. Varma and Kathryn S. Thomas
NACE: Corrosion and Metallurgy
XXI International Materials Research Congress
Cancun, Mexico, August 14, 2012

28. "A Comparison of Static and Cyclic Long Term Oxidation of Two Nb-Cr-Mo-Si-B Alloys"
Kathryn Thomas and S.K. Varma
Beyond Nickel-Base Superalloys-II
Pittsburgh, Pennsylvania, October 9, 2012

	Name	Degree	Status
	Graduate Students		
1	Julieta Ventura	M.S.	NASA, Houston, TX
2	David Alvarez	M.S.	Owns Silver Mine in Mexico
3	Benedict Portillo	M.S.	Finished M.S.
4	Benedict Portillo	Ph.D.	Employed
5	Clemente Parga	M.S.	Working on Ph.D. in France
6	Daniel Brendan Voglewede	M.S.	Halliburton, Houston, TX
7	Nydia Esparza	M.S.	Oneok, Tulsa, OK
8	Victoria Rangel	M.S.	Alcoa, Wichita Falls, TX
	Undergraduate Students		
1	Arianna Acosta	B.S.	Employed
2	Krista Amato	B.S.	Working for Ph.D. at UTEP
3	Jennifer Hernandez	B.S.	Working for Ph.D. at UTEP
4	Kimberline Schnittker	B.S.	M.S. at UTEP

5	Sylvia Natividad	B.S.	Finished M.S.
6	Amanda Gutierrez	B.S.	Working for Ph.D. at UTEP
7	Brenda Arellano	B.S.	M.S. at UTEP
8	Kathryn Thomas	B.S.	Working for Ph.D. at UTEP

L to R Nydia Esparza, Amanda Gutierrez, Kathryn Thomas, Daniel Brendan Voglewede, Brenda Arellano, Ruth Dasary, Victoria Rangel